INL/EXT-11-23391

Further Evaluation of the Neutron Resonance Transmission Analysis (NRTA) Technique for Assaying Plutonium in Spent Fuel

J. W. Sterbentz
D. L. Chichester

September 2011

INL is a U.S. Department of Energy National Laboratory operated by Battelle Energy Alliance

INL/EXT-11-23391

Further Evaluation of the Neutron Resonance Transmission Analysis (NRTA) Technique for Assaying Plutonium in Spent Fuel

J. W. Sterbentz
D. L. Chichester

September 2011

Idaho National Laboratory
Idaho Falls, Idaho 83415

http://www.inl.gov

Prepared for the
U.S. Department of Energy
Office of National Nuclear Security Administration
Under DOE Idaho Operations Office
Contract DE-AC07-05ID14517

ACKNOWLEDGEMENT

The authors would like to acknowledge and thank Dr. Steve Tobin of Los Alamos National Laboratory for his assistance in coordinating and integrating the NRTA technique into the NGSI spent fuel assay project and in allowing us access to the LANL resources developed to support spent-fuel assay research and development. The work in this report was sponsored by the National Nuclear Security Administration Office of Nonproliferation and International Security (NA-241).

EXECUTIVE SUMMARY

This is an end-of-year report (Fiscal Year (FY) 2011) for the second year of effort on a project funded by the National Nuclear Security Administration's Office of Nuclear Safeguards (NA-241). The goal of this project is to investigate the feasibility of using Neutron Resonance Transmission Analysis (NRTA) to assay plutonium in commercial light-water-reactor spent fuel. This project is part of a larger research effort within the Next-Generation Safeguards Initiative (NGSI) to evaluate methods for assaying plutonium in spent fuel, the *Plutonium Assay Challenge*. The second-year goals for this project included: 1) assessing the neutron source strength needed for the NRTA technique, 2) estimating count times, 3) assessing the effect of temperature on the transmitted signal, (4) estimating plutonium content in a spent fuel assembly, (5) providing a preliminary assessment of the neutron detectors, and (6) documenting this work in an end of the year report (this report). Research teams at Los Alamos National Laboratory (LANL), Lawrence Berkeley National Laboratory (LBNL), Pacific Northwest National Laboratory (PNNL), and at several universities are also working to investigate plutonium assay methods for spent-fuel safeguards. While the NRTA technique is well proven in the scientific literature for assaying individual spent fuel pins, it is a newcomer to the current NGSI efforts studying Pu assay method techniques having just started in March 2010; several analytical techniques have been under investigation within this program for two to three years or more. This report summarizes work performed over a nine month period from January-September 2011 and is to be considered a follow-on or add-on report to our previous published summary report from December 2010 (INL/EXT-10-20620).

Preliminary results indicate that NRTA has great potential for being able to assay intact spent fuel assemblies. It can identify four plutonium isotopes (^{239}Pu, ^{240}Pu, ^{241}Pu, and ^{242}Pu), three uranium isotopes (^{235}U, ^{236}U, and ^{238}U), and six resonant fission products (^{99}Tc, ^{103}Rh, ^{131}Xe, ^{133}Cs, ^{145}Nd, and ^{152}Sm). It can determine the areal density or mass of these isotopes in single- or multiple-pin integral transmission scans. Multiple, difficult-to-hoax observables exist to allow the detection of material diversion (pin defects) including fast-neutron and x-ray radiography, gross transmission neutron counting (uranium-oxygen macroscopic cross-section spoofing), plutonium absorption analysis (plutonium diversion), and fission-product resonance absorption analysis (analysis of fission product ratio agreement with both declared and measured/verified fuel burn-up). Initial benchmark modeling has shown excellent agreement with previously published experimental data for measurements where plutonium assays were experimentally demonstrated to have a precision of better than 3%. Analyses of full 17 × 17 pressurized water reactor (PWR) fuel assembly arrays, of varying initial enrichments, cooling times, and burnups, suggest a scale-up of the NRTA technique is possible while still maintaining a measurement precision in the 1% to 4% range. The results suggest sufficient transmission strength and signal differentiability is possible for assaying up to 8-pin rows. For an 8-pin maximum assay (looking at diagonal slices of an assembly), 64% of the fuel pins in an assembly can be directly part of integral transmission assay measurements. Collimated neutron beams or two-dimensional neutron detectors that can spatially resolve a fuel pin diameter have the potential to assay roughly the outer one-third of a pin lineup for up to 12-pin rows. For a 12-pin maximum,

100% of the fuel pins in an assembly can be part of one or more integral transmission assay measurements.

The NRTA technique requires an intense pulsed-neutron source on the order of 8.0×10^{12} n s^{-1} (4π emission); this source strength will permit reasonable assay counting times for a 17 × 17 PWR spent fuel assembly. For example, a single-pin assay would require only 3 minutes and an 8-pin assay approximately 45 minutes. Although the required source is relatively intense, there are several charged-particle accelerator systems that could be used for the NRTA technique with current commercial-level technology. In this report a linear electron accelerator (linac) is used for our assessments but other accelerators such as proton accelerators could be used as well. A 30-MeV linac system could be optimized to achieve the desired 8.0×10^{12} n s^{-1} source strength.

Also part of the FY2011 effort was work to perform a calculational transmission assay of a 17 × 17 PWR spent fuel assembly (45 GWD/MTU burnup). Time-of-flight neutron transmission spectra were generated for rows of pins ranging from 1 to 12 pins. Using a single ^{239}Pu resonance (10.93 eV), simple attenuation analysis was used to assess the ^{239}Pu mass in each of the assays pin rows. Assuming the NRTA technique is capable of assaying up to 8-pin rows, the NRTA-estimated total ^{239}Pu was within 4% of the known ^{239}Pu assembly mass per the LANL spent fuel library inventory. For a 12-pin scan capability, every pin in the assembly could be part of one or more integral scans; in this approach multiple scan information for the same pins could be unfolded to potentially allow the determination of ^{239}Pu mass values for sub-regions of the assembly. Further, the mass estimate accuracy could be greatly improved, perhaps to the 1-2% level, upon the development of more sophisticated computer analysis tools that could correct the transmission spectra for resonance overlap/interference and hidden resonance within the actinide or fission product resonance of interest.

CONTENTS

FIGURES

TABLES

Further Evaluation of the Neutron Resonance Transmission Analysis (NRTA) Technique for Assaying Plutonium in Spent Fuel

1 INTRODUCTION

This report documents work performed by Idaho National Laboratory (INL) over the nine-month period from January through September, 2011. This work focused on further evaluation of the non-destructive assay technique known as neutron-resonance transmission analysis (NRTA) for quantifying plutonium in spent nuclear fuel. The 2011 work documented here is an extension to the work performed at INL on this topic in 2010.[1]

The first phase of this project was focused primarily on conceptual studies to assess the viability of the NRTA technique as a possible means to assay a spent pressurized water reactor (PWR) fuel assembly to determine its plutonium content. With the viability of the NRTA technique established in the first phase, the second phase of the NRTA project (2011 work) focused on answering questions related to neutron source strength, count times, and estimation of the plutonium content in a spent PWR assembly. This project has been sponsored by the National Nuclear Security Administration's Next Generation Safeguards Initiative and is a part of a larger set of investigations aimed at identifying and studying nondestructive methods for assaying spent fuel.[2]

1.1 Background

New analytical methods are needed to assay spent nuclear fuel and determine fissile material inventories. Ideally, these measurements will be able to assay whole, unaltered commercial-nuclear-reactor assemblies without the need for disassembly, sectioning, or chopping, providing “head-end” inventory data for materials entering current-generation and future spent-fuel reprocessing/recycling facilities. Quantitative measurements of plutonium entries into safeguarded fuel reprocessing facilities prior to material decomposition will provide a higher level of confidence for the actual plutonium mass than found with the current approach, which relies on vendor-supplied burn-up calculations. One potential method to accomplish this task is neutron resonance transmission analysis, NRTA.

The NRTA concept is based on solid theoretical principles, has been demonstrated experimentally at the bench scale using commercial spent fuel, and has achieved a plutonium assay measurement precision of 2-4% in ad-hoc testing.[3-5] The technique uses a pulsed accelerator to produce an intense, short pulse of neutrons. These neutrons, traveling at different speeds according to their energy in a time-of-flight (TOF) configuration, are used to interrogate a spent fuel assembly. Neutron transmission through the assembly is monitored as a function of neutron energy (time after the pulse), similar to the way neutron cross-section data is often collected. Neutron detection is performed using a high-rate sensor, such as a lithiated-glass scintillation detector.[4-6] Results are read from the detector as count rate versus time, with faster (higher-energy)

neutrons arriving first and slower (lower-energy) neutrons arriving later. The low-energy elastic scattering and absorption resonances of plutonium and other isotopes modulate the transmitted neutron spectrum. The plutonium content in the fuel can be determined by analyzing this attenuation. The data format is similar to that from a Lead Slowing-Down Spectrometer (LSDS).[7] However, unlike in LSDS measurements the fuel does not play an important role in the neutron thermalization process. Unknown material impurities from hydrides (hydrogen diffusion into cladding metals) or extreme fission product loadings (which may be present in advanced high-burnup mixed-oxide or minor-actinide bearing fuels) in the spent fuel will not detrimentally alter the neutron source-term energy distribution in a way that impacts the NRTA measurement.

1.2 History

The NRTA concept is not new. The first paper (reference 8) on the subject was published in 1975, followed by substantial research through the mid-1980s. Most of the published research literature is from the National Bureau of Standards (NBS); many of these NBS papers are cited in this report. Much of the published literature is focused on applications related to neutron radiography, in particular, the measurement of uranium in waste materials and the assay of isotopic heterogeneities in welds, brazes, and metals.[9-14] One NRTA study looked at optimizing the accelerator neutron output.[15] Before NRTA research and publishing literature diminished, around 1984, several papers documented the use of NRTA to characterize a PWR spent fuel pellet, a pellet with approximately 25 GWD/MTU burnup.[3-5] These four NRTA spent-fuel papers have provided confirmation that the NRTA concept is a viable and potentially very powerful spent assay technique.

These same four NRTA spent-fuel papers provide important benchmark data that is used here to provide a level of validation with MCNP-calculated transmission spectra, providing justification for the use of the MCNP computer code, models, cross-section data, and calculated results in this report. The MCNP code and models have been used to assess the important question of what is the maximum number of PWR fuel pins the NRTA technique can penetrate and assay. Plus, the calculations have been extremely useful in addressing other issues, including: (1) identifying which resonance depressions corresponded to which spent-fuel isotopes, (2) understanding the effects of assembly burnup and cooling time on NRTA measurements, (3) establishing the impact of spent-fuel assembly neutron emission on the NRTA signal background and how to minimize this effect, and (4) limitations of the NRTA technique. The conceptual study calculations have also provided a basis for developing a preliminary NRTA system design with emphasis on the minimization of the size of the NRTA physical footprint.

1.3 Status

In December 2010 INL submitted a technical report summarizing the first year's activity and progress in the effort to evaluate the feasibility of using NRTA to address the spent fuel plutonium assay challenge of the Next Generation Safeguards Initiative (NGSI).[1] The second year's activities started in January 2011 and ended in September 2011 and are documented in this report. In May 2011, the INL team prepared a technical presentation for a technical review committee assembled by S. Tobin (Los Alamos National Laboratory,(LANL)) for the NA-241. The review committee reviewed all 14

NDA techniques and provided an evaluation report with the techniques ranked and rated against one another for an eventual down select. The NRTA technique did not make the down select and was not given FY2012 funding to continue the effort.

INL presented a technical paper on the NRTA technique to the Institute of Nuclear Materials Management (INMM52) conference in July 2011. The INL NRTA project has made good progress in the technical assessment and has shown the NRTA technique to be a viable and potentially high-accuracy plutonium assay technique.

2 NRTA TECHNIQUE

This section provides a basic discussion of the NRTA concept and underlying physics.(This section is taken from reference [1]).

2.1 Basic Concept

The NRTA technique uses low-energy neutrons as the probing radiation. The low-energy neutrons are thermal and epithermal neutrons in the 0.1-40 eV energy range. This neutron energy range is at the bottom end of the actinide-resonance range, where most actinides have at least one or more resonances. For the spent fuel actinides, as will be seen, the resonances are typically large in magnitude, narrow in breadth, and fortuitously well-separated resulting in distinctive resonance transmission spectra.

Of the hundreds of fission-product isotopes found in spent fuel, only a half-dozen or so have any resonance structure in the 0.1-40 eV energy range. Each of these fission products has only one resonance in this energy range, none interfere with the actinide resonances. All the other isotopes present in the spent fuel – for example, oxygen in the UO_2 and zirconium, tin, iron, chromium, oxygen, niobium, nickel, carbon, and silicon in the Zircaloy-4 clad – also have no resonance structure in the 0.1-40 eV range and, therefore, also do not interfere with the resonance transmission signal. The same is true for the hydrogen impurity (hydration) in the clad and air isotopes.

The low-energy neutrons used for NRTA measurements are generated in a complex multi-step process that starts with a pulsed high-energy particle accelerator, such as a linac. In the electron accelerator approach, high-energy electrons impact a high-Z converter (e.g., tungsten or tantalum) and produce a continuum of bremsstrahlung photons. It is practical to consider using an accelerator having an endpoint energy in the range of 12 MeV for this discussion. The high-energy bremsstrahlung photons (2-12 MeV) then pass through a low-Z photo-neutron converter (heavy water or beryllium) to produce high-energy neutrons. These high-energy neutrons pass through a low-Z neutron moderator (polyethylene, light water, or heavy water) where they scatter and lose energy, a process called thermalization. This scattering process yields a continuous distribution of neutrons, varying in energy from the starting energy down to approximately 0.025 eV, the thermal kinetic energy of nuclei. It is the portion of the continuum having thermal and epithermal neutrons from 0.1 to 40 eV that is of interest to the NRTA technique.

The thermalized neutrons can then be collimated to create a neutron beam that is directed at a spent fuel assembly. A fraction of the neutrons incident on the fuel assembly scatter out of the beam as they interact with individual fuels pins in the

assembly through low-energy elastic scattering, neutron-capture absorption, and neutron-capture fission. The rest of the neutrons pass through the spent fuel assembly unaffected as the transmitted signal. It is these transmitted neutrons – the modulated beam – that is measured in the NRTA technique. The modulated beam, or transmitted signal, is an integral scan of rows of pins in the assembly and is analogous to how a traditional x-ray radiograph is used to detect the presence of dense objects in the human body (bones) and the location of low density regions (bone cracks). The NRTA technique does not assay individual pins with the exception of the four corner pins.

Many advances have been made between the early 1980s and today. These advances help enable practical modeling and, potentially, the implementation of the NRTA technique. The most significant enabling advances have been improvements in the nuclear data needed to analyze NRTA data; neutron cross sections and resonance parameters have been re-measured and evaluated and are now known with a high degree of accuracy. The NRTA technique grew out of cross-section measurement techniques; it is basically the inverse to the problem of measuring neutron cross sections. In the case of neutron cross-section measurements, the two known variables are (1) the sample isotopic content, or sample areal density N_i and (2) the transmission flux T_i through isotope i from the TOF measurement. The third variable, the total cross section σ_{ti} for a isotope i, is the unknown variable and the desired quantity to be measured. The total cross section is then calculable as a function of neutron energy, E, from Eq. 1.

$$T_i(E) = e^{-N_i \sigma_{ti}(E)} \qquad \text{Eq. 1}$$

For NRTA, the unknown variable is the isotopic areal density N_i, and the two known variables are the total cross section σ_{ti} and the measured neutron transmission flux T_i. The same formula above is then used to calculate the areal density. Other known factors include the fuel pin and assembly geometry and dimensions, cladding material, and the fuel form (UO_2). Knowledge of these "other" factors should significantly reduce the systematic error, improve the overall NRTA measurement accuracy, and promote the use of calibration standards.

Calibration standards will play an important role in the assessment of the first NRTA system, but also in all subsequent spent fuel measurements to calibrate the system, establish biases, and reduce systematic error. Combinations of pins and assemblies with known dimensions and material compositions can be used as calibration standards. For example, pins containing (1) no fuel, (2) fresh UO_2 with 100% ^{238}U and various ^{235}U enrichments, (3) and spent fuel surrogate compositions (uranium, plutonium, and fission product isotopes) can all be fabricated with accurately known isotopic compositions.

High-fidelity burnup calculations can also play an important role and further support NRTA spent-fuel transmission measurements. NRTA transmission measurements can be compared to calculated transmission measurements. Agreement between measured and calculated spectra, and then comparison of the corresponding isotopic concentrations, can be used to confirm pin/assembly isotopic concentrations, burnup, and cooling times.

2.2 System Components

The major components of an NRTA system include: (1) a linear electron accelerator capable of pulsed operation, (2) converter, photoneutron targets, filters, collimators, and shielding, (3) time-of-flight drift tube, (4) vertical chamber to contain and cool a spent fuel assembly, (5) mechanism to lift, rotate, and transversely move the assembly, and (6) neutron detectors with associated TOF electronics for data acquisition (such as a multichannel scalar (MCS) configuration). Figure 1 shows a cartoon of the basic NRTA concept and component layout with preliminary material and accelerator parameters.

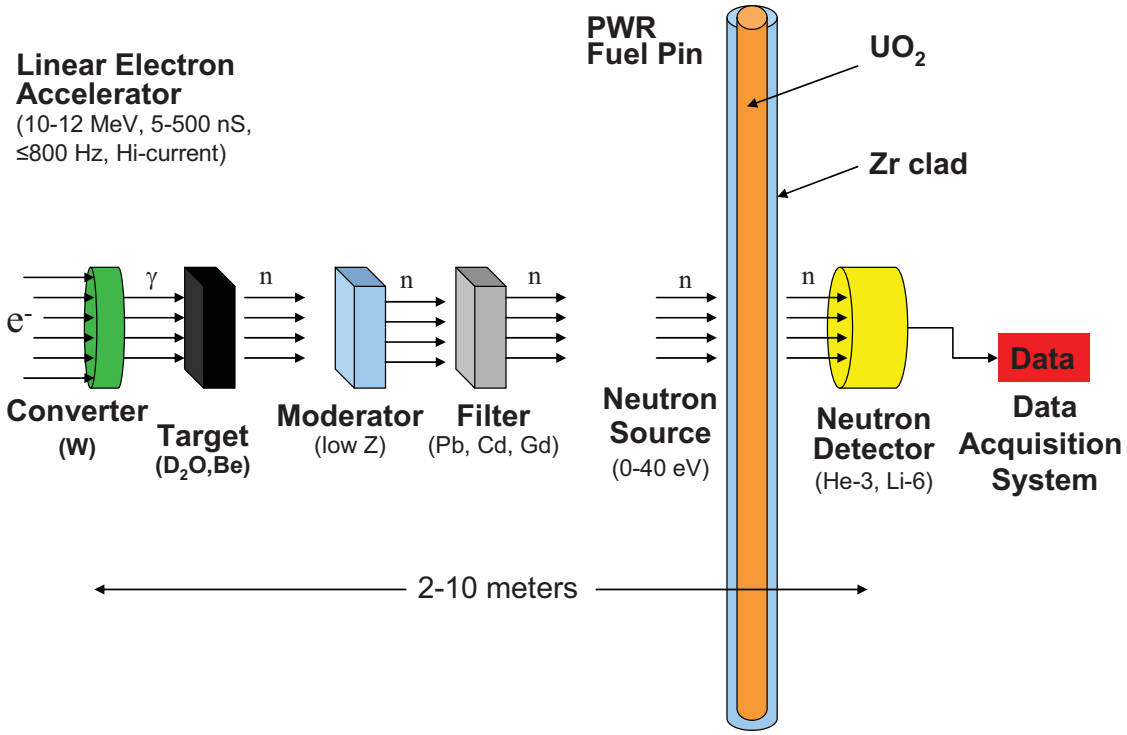

Figure 1 Basic NRTA concept and component layout.

The neutron time-of-flight (TOF) method, with a precisely known flight-tube length, will be used to measure the transmission neutron energies. Neutron detection is performed using a high-rate sensor, such as a helium-3 proportional counter or lithiated-glass scintillation detector. Results are read from the detector as counts versus time, with faster neutrons (higher-energy neutrons) arriving first and slower neutrons (lower-energy neutrons) arriving later.

The low-energy fission, capture, and elastic scattering resonances of plutonium and other isotopes modulate the transmitted-neutron spectrum. Spectrum modulation, or neutron attenuation, appears as depressions in the collected data that correspond to energy-specific resonances and, hence, specific and identifiable isotopes. The plutonium content in the fuel can be determined by analyzing the appropriate depression signals (magnitude or area of the depression).

The NRTA technique will require transmission measurements with and without the spent fuel assembly. A transmission measurement without the assembly is needed to provide a baseline measurement, or the unperturbed transmission flux spectrum, from which the actinide-resonance flux depressions are measured. A transmission measurement of rows with multiple pins can result in significant out-scatter of neutrons from the transmission signal. Calibration standards could be used to measure the individual loss effects due to the clad, oxide, and ^{238}U. The bulk of the signal loss is due to ^{238}U and the oxide. Adding these signal components to the measured signal would allow the reconstruction of a transmission signal due to the lower concentration actinides and fission products alone, which may improve measurement accuracy.

A PWR assembly assay will require many transmission measurements for a complete assay. In order to accommodate multiple integral assay measurements, the PWR fuel assembly will need to be rotated about its central axis and moved transversely across the neutron interrogating beam. Rotation and transverse movement will allow assay of both the straight and diagonal rows of pins (Figure 2). A full assembly assay would require four 90-degree rotations. Many of the fuel pins will be assayed multiple times during the process as part of different integral row transmission measurements. Due to assembly geometry and burnup symmetry, quadrant assays should be similar, and any deviations between quadrant assays could be treated as a potential diversion.

The NRTA technique is envisioned to assay rows of in-line pins and to produce an integral value for the uranium, plutonium, and fission-product concentrations. Exceptions are the four corner pins in the fuel assembly. The NRTA technique will be able to analyze these four pins individually and to determine the uranium, plutonium, and fission-product concentrations most accurately. These corner-pin measurements could be compared to calculated values from high-fidelity burnup calculations and thereby allow for verification of an assembly burnup and cooling time. Subsequent NRTA measurements of the assembly's multiple pin rows (2-12 pins per row) should then also be agreement with the burnup predictions.

3 NUMERICAL SIMULATIONS

This section provides information on the numerical computer code simulations used to perform the conceptual studies, also referred to as feasibility studies.

3.1 Computer Codes

Both the MCNP5 and MCNPX computer codes were used in the numerical simulations presented here.[16,17] Both codes gave statistically the same results but because the codes resided on different computer systems at INL code usage was based on computer system availability. The models were interchangeable.

3.2 MCNP Models

Several MCNP models were developed for the feasibility studies but all were relatively simple in geometry. The simplest geometry models included a directed neutron source, a single fuel pin or line of pins, vacuum flight tube, and flux detector cells. More

sophisticated models include a complete PWR 17 × 17 pin assembly; the assembly model was taken directly from the LANL 64 library data/models.[18]

The MCNP models used one or more PWR fuel pins in a row. The PWR spent-fuel pin geometry was based on the LANL 64 spent fuel library, namely, a 0.82 cm UO_2 pellet diameter, 0.95 cm diameter clad (no gap), and fuel pin pitch of 1.26 cm. INL MCNP models developed prior to the adoption of the LANL models used similar but slightly different pin-cell dimensions, or a 0.819 cm UO_2 pellet diameter, 0.0082 cm gap, 0.9498 cm diameter clad, and pin pitch of 1.25 cm.

In all MCNP models the neutron source was uniformly sampled over the desired transmission neutron-energy range. In an actual physical NRTA system a slowing-down neutron source would be expected to exhibit some non-uniformity, in particular, slightly higher flux at higher energies. In the 0-40 eV energy range, with the use of a low-Z neutron moderator with low absorption, a relatively flat and uniform energy-flux distribution would be expected. Also, the benchmark data does not exhibit a significant flux tilt to higher energies.

The MCNP models also used two different beam geometries: cylindrical beam and directed point-source beam. The cylindrical beam typically had a diameter less than the UO_2 pellet diameter (<0.82 cm) and was directed through the fuel pin center, such that no neutrons struck the detector flux tally cell without first passing through the UO_2 pellet. The cylindrical-beam radius was also varied for some studies. The directed point source is essentially a cylindrical beam with zero radius: a point source directed in a particular direction creating a line of neutrons. The directed point source is useful in order to assess the effect of pellet curvature on the transmission signal.

3.3 Nuclear Data

Evaluated Nuclear Data File VII (ENDF-7) was used in the numerical simulations.[19]

3.4 LANL Spent Fuel Library

Los Alamos National Laboratory has provided the NGSI working group a comprehensive set of PWR spent-fuel-assembly models, complete with individual spent-fuel material compositions for each pin.[18] Three distinct libraries were created for assemblies in air, water, and borated-water. Each of the three libraries included 64 individual spent fuel assemblies, covering the parametric variable space of (1) initial uranium enrichments of 2, 3, 4, and 5 wt% ^{235}U, (2) burnups of 15, 30, 45, and 60 GWD/MTU, and (3) cooling times of 1, 5, 20, and 80 years. The LANL PWR assembly model assumes both quadrant symmetry and symmetry within a quadrant where certain groups of pins have identical burnup. These assumptions allow the 264 total possible fuel pin burnups in the 17 × 17 pin array to be reduced to 39 unique pin burnups. Each of the 39 unique burnup pins, however, had four radial burnup zones. Therefore, each of the 64 LANL libraries had a total of 4 × 39 = 156 fuel compositions, using 4 radial material compositions for each of the 39 unique burnup pins in the assembly. Uniform axial burnup was further assumed for each pin radial zone.

The NRTA work here used only the 64 library set for "assembly in air" since the NRTA technique will require the spent fuel assembly to be assayed either in vacuum or air.

3.5 PWR Fuel Assembly

A PWR fuel assembly was chosen as the basis for which all NGSI assay techniques would be evaluated. This particular fuel assembly design is a 17 × 17 array with 264 fuel pins and 25 guide tubes. The fuel pins and guide tubes are symmetrically arranged such that each assembly quadrant is a mirror-image of an adjacent quadrant. For NRTA calculations the 25 guide tubes are assumed to be voided or air-filled; the central pin location in the assembly is a guide tube. Fuel pins consist of a UO_2 pellet (0.82 cm diameter) and a Zircaloy-4 clad tube (0.95 cm diameter). The Zircaloy-4 guide tube was assumed to be 1.142 cm in diameter with a wall thickness of 0.042 cm. The pin pitch was 1.26 cm and the overall 17 × 17 array had the dimensions of 21.42 × 21.42 cm. The fuel rods had a length 365.76 cm (12 ft).

Figure 2 shows a cross sectional view of PWR 17 × 17 fuel assembly. The 25 large white circles in the assembly are the guide tubes (air-filled), the remaining colored circles represent the fuel pins. Nine (9) vertical lines are drawn over the left half of the assembly and the center row (row 9). In addition, 17 diagonal lines are drawn over the lower half the assembly. At the end of each line is the number of fuel pins in that line. Note that the guide tubes are not counted in the line totals.

The pin totals in Figure 2 range from 1–17. Of the 17 possible vertical lines (only 9 shown in the figure), 3 lines would have 12 pins, 2 lines 14 and 15, and 10 lines 17. The 3 lines with 12 pins are noteworthy because they are centrally-located, each line containing 5 guide tubes. For the 17 diagonal lines, only 3 lines have more than 12 pins. It can be shown for the PWR 17 × 17 assembly that, if the NRTA technique can assay 12 pins in a row in a single integral transmission measurement, then every pin in the assembly can be part of one or more integral transmission measurements; complete assay coverage of all the assembly pins would then be possible.

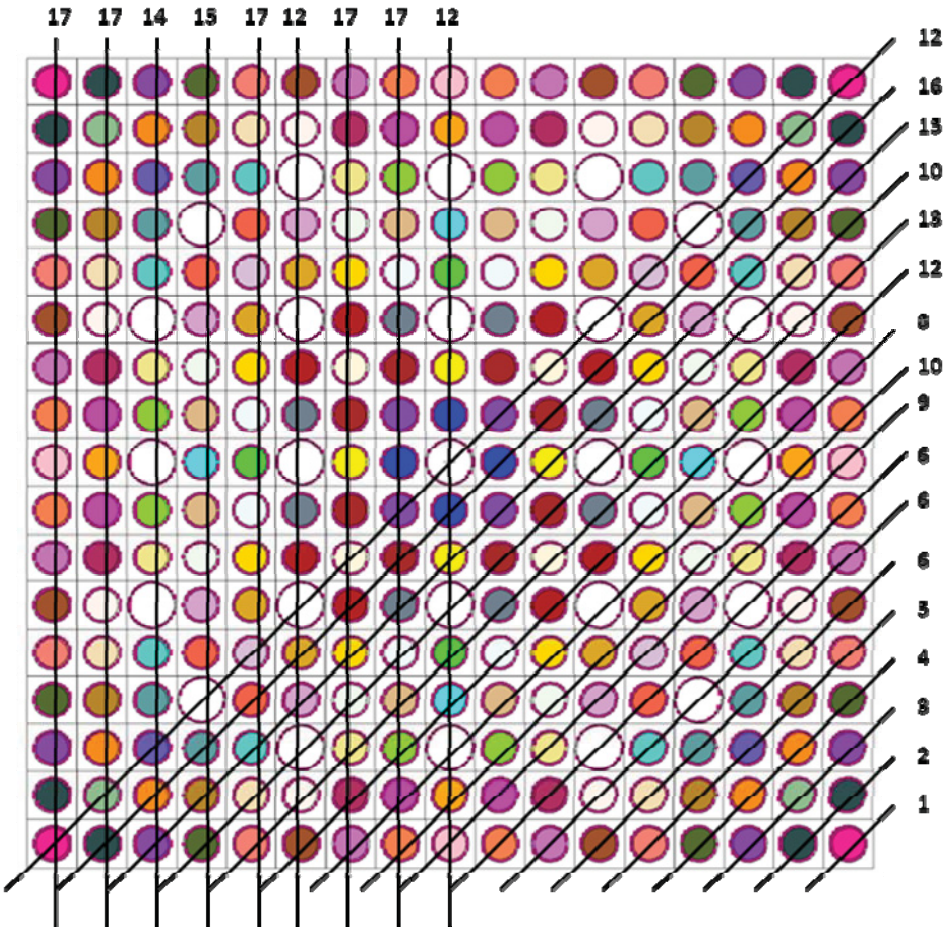

Figure 2 PWR 17 × 17 fuel assembly showing number of fuel pins in the vertical columns and diagonal lines.

4 CONCEPTUAL STUDIES

This section presents preliminary conceptual studies which include: 1) assessing the neutron source strength needed for the NRTA technique, 2) estimating count times, 3) assessing the effect of temperature on the transmitted signal, (4) estimating ^{239}Pu content in a spent fuel assembly, and (5) providing a preliminary assessment of the neutron detectors. These studies are an extension of the conceptual studies performed in FY2010. All calculated results are all based on the MCNP code, MCNP transmission models, and MCNP ACER neutron cross-section library data which is in turn derived from ENDF-7 nuclear data.

4.1 Neutron Source Strength

Neutron source strength is an important parameter for the NRTA technique. Transmitted signal intensity and resolution as well as count times are all directly dependent on the neutron source strength. For the PWR assembly, where our goal is to assay the entire assembly, significant signal attenuation can be expected for rows of pins

with more than 8 pins; the greater the attenuation, the longer the count time and consequently the greater the neutron source strength required.

It was anticipated that a relatively intense neutron source would be required to achieve reasonable count times. Estimates on the order of 10^{12} n s^{-1} (4π emission) were projected due to the basic physics of the NRTA technique and the results of the 2010 conceptual studies. Inherent neutron losses from source-to-detector include: (1) isotropic neutron emission from the converter targets and the corresponding $1/r^2$ loss over a 5-m long flight tube to the neutron detectors, (2) deliberate slowing down of a only a fraction of the emitted hard spectrum neutrons, (3) and then use of only a fraction of the slowed down neutrons, or neutrons of energy 0.1-20 eV, (4) neutron transmission losses due absorption and scattering through the PWR assembly pins, and (5) losses due to neutron detector efficiency. In order to accept these losses and achieve sufficient detector counts and consequently reasonable count times, the neutron source strength needed to be estimated for the NRTA technique and the preliminary system design.

The estimate of the required neutron source strength needed for an operating accelerator system was selected based on published operating parameters and neutron emission rates previously achieved at comparable facilities. For this effort a linear electron accelerator was chosen due to the large published literature database. Three low-energy (<10 MeV) electron linear accelerator systems were selected [20,21,22]. These three systems were modeled using MCNP and neutron flux, spectra, and emission rates calculated and compared to the published results. The goal was to later use these models to optimize the neutron emission rates and scale-up the operating parameters as needed to achieve a desired (higher) neutron emission rate.

In the past, high-energy linear electron accelerators (100 MeV) were most often used for neutron cross section measurements and the few proof-of-principle tests for NRTA. It is therefore known that a high-energy electron accelerator could be successfully employed for NRTA application. In addition, it was our intent to explore the possibility of using an accelerator system specifically geared for an NRTA application, which meant possibly using a high-current, low-energy electron in which the accelerator power was directed to producing copious amounts of low-energy electrons versus fewer high energy electrons that would need to be slowed-down to lower energies for NRTA usage. We based our decision on a published technical paper suggesting such a possibility.[15]

The use of low-energy electrons (≤10 MeV) necessitates the use of either beryllium or heavy water (deuterium) as the photon-to-neutron converter material, because these two practical materials have the lowest neutron binding energies; the binding energies for beryllium and heavy water are 1.67 and 2.22 MeV, respectively. Use of low-Z materials like beryllium and heavy water also provide the advantage that they can also slow down the photoneutrons to thermal and epithermal energies and reduce or possibly eliminate the need for a dedicated low-Z slowing down converter required in high-energy systems. In addition, the production of lower energy neutrons means the accelerator power is not wasted on high-energy neutrons lost in 4π emission.

The three benchmark accelerator systems were specifically selected because of their use of low-energy electrons (<10 MeV), use of beryllium or heavy water photon-to-

neutron converters, sufficient system description for modeling, and published neutron emission rates. Comparison of the calculated and measured values provided a means to verify the MCNPX code/model/cross section data. Table 1 gives the measured neutron emission rates along with the corresponding calculated MCNPX results for the three benchmark accelerator systems. The last column gives the high-Z electron-to-photon converter material along with the photon-to-neutron converter material used; system dimensions and operating accelerator parameters are given in the published papers.

Table 1 Measured and calculated neutron emission rates for the three benchmark accelerator systems.

Reference	Electron Energy [MeV]	Measured [n s^{-1}]	Calculated	System Description
Lakosi [20]	4.0	$\sim 1.0 \times 10^{9}$ n s^{-1}	0.86×10^{9} n s^{-1}	Pt/D_2O
Eshwarappa [21]	8.75	2.25×10^{9} n s^{-1}	1.96×10^{9} n s^{-1}	Ta/Be
Auditore [22]	5.0	6.25×10^{-8} n cm^{-2} e^{-1}	5.49×10^{-8} n cm^{-2} e^{-1}	W/Be

From Table 1, it is clear that measured results are all in good agreement with the MCNPX calculated results, which provided confidence in the use and implementation of the MCNPX code, models, and cross section data. The Auditore model was chosen as our model base, modifications were then made to this base model for NRTA application. These modifications included: (1) 10 MeV electron energy, (2) use of an optimal tungsten thickness (0.145 cm) (per reference [23]), and (3) a 5-m flight tube. The flight tube was added to the model in order to calculate the neutron flux at the end of the flight tube (location of the neutron detectors). The calculated neutron emission rate for the modified base model produced a 2.7×10^{11} n s^{-1} (4π) neutron emission rate for the accelerator operating with a hypothetical average beam current of 100 μA and beryllium cylinder target (28-cm diameter and 14-cm length). The 2.7×10^{11} n s^{-1} source strength is used in the following section "Count Time Estimates" to estimate count times for multiple pin row assays of a PWR assembly.

Although we have assumed that the NRTA neutron source would be based on a linear electron accelerator producing bremsstrahlung photoneutrons, other nuclear reactions and accelerator systems could be used as well. For example, accelerators using protons or deuterons on a variety of materials can also be useful neutron sources. Figure 3 gives neutron yield (n s^{-1} μA^{-1}) as a function of energy for some different nuclear reactions.[24,25]

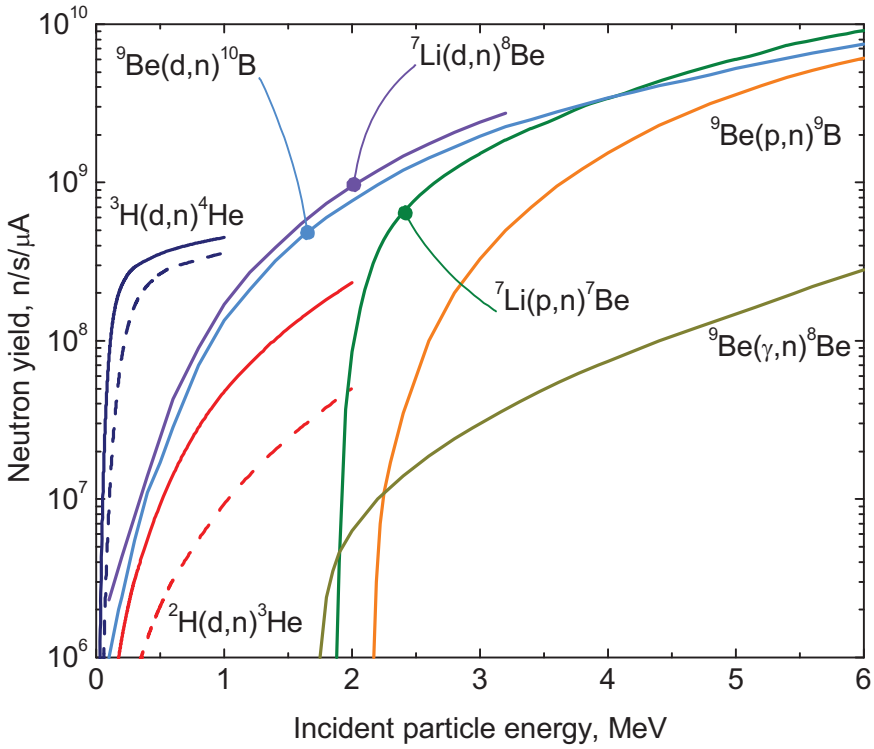

Figure 3 Neutron yields achievable from different light-ion, accelerator-based neutron sources.[24,25]

The following are examples of other nuclear reactions that could be used as potential neutron sources for NRTA, including a 35 MeV bremsstrahlung source for comparison:

1. ^{7}Li(p,n)Be^{7}, E_p = 2.0 MeV, Y ≈ 1.0 × 10^{11} n s^{-1} mA^{-1}
2. ^{7}Li(p,n)Be^{7}, E_p = 2.5 MeV, Y ≈ 8.8 × 10^{11} n s^{-1} mA^{-1}
3. ^{9}Be(p,n)B^{9}, E_p = 11.0 MeV, Y ≈ 2.2 × 10^{13} n s^{-1} mA^{-1}
4. Bremsstrahlung (γ,n), E_e = 35.0 MeV, Y ≈ 5.6 × 10^{13} n s^{-1} mA^{-1}

Specific examples of the use of these reactions at accelerator facilities include [26]:

1. Compact Pulsed Hadron Source, Tsinghua University, China
   E_p = 13.0 MeV, I_{ave} = 1.25 mA, R=50 Hz
2. Low energy neutron source, Indiana University, U.S.
   E_p = 13.0 MeV, Y ≈ 4.2 × 10^{13} n s^{-1}
3. KUURI-FFAG, Kyoto University, Japan
   E_p = 11.0 MeV, Y ≈ 5.0 × 10^{13} n s^{-1}, R=200 Hz, PW=200μs
4. KUURI-eLINAC, Kyoto University, Japan
   E_e = 30.0 MeV, Y ≈ 8.0 × 10^{12} n s^{-1}, I_{ave} = 200 μA, R=300 Hz

It is clear that there are multiple neutron source options available today for the NRTA technique. Current state-of-the-art technology can produce neutron yields of 5 × 10^{12} n s^{-1}, which is sufficient for an NRTA high intensity neutron source. Cost, of course,

is a significant factor for all high-yield accelerator-based SNF assay systems but infrastructure costs will most likely be the primary driving factor. Handling spent fuel is an expensive proposition.

4.2 Count Time Estimates

This section provides count time estimates to achieve sufficient detector transmission signal and number of counts for use in an NRTA assay determination. The count time estimate analysis uses the previously derived neutron source strength value of 2.7×10^{11} n s^{-1} (4π emission) calculated using the modified W/Be base model from the previous section on "Neutron Source Strength". Count times are estimated for a single PWR pin transmission as well as an 8-pin row transmission which covers the range of 1-8 pin row assays.

The following assumptions are used in the count time estimates:

1. Linear electron accelerator with maximum electron energy of 10.0 MeV,
2. Optimal tungsten converter thickness of 1.45 cm for 10 MeV operation,
3. Neutron energy range of interest: 1.0—20 eV,
4. Tungsten-beryllium (W/Be) converters using Auditore dimensions,
5. 5-meter flight tube distance to detectors,
6. 100 μA average beam current,
7. Detector active area of π cm^2 (1 cm radius) perpendicular to beamline axis,
8. Neutron detector efficiency $\varepsilon = 20\%$.

Under these assumptions, the accelerator system will emit 2.7×10^{11} n s^{-1}. At a 5-meter distance away and over an assumed detector active area of 3.14 cm^2 (r = 1 cm), a neutron current of 592 n s^{-1} in the 1-20 eV energy can be expected across the detector area. The modeling results have shown that the neutrons are relatively evenly distributed over this relatively narrow 1-20 eV energy range. If we then divide the 1-20 eV energy range into fine energy bins (count bins) of width 0.05-eV, this will give us (20-1) ÷ 0.05 = 380 energy bins. The number of neutrons per bin is 592 ÷ 380 = 1.56 n s^{-1} bin^{-1}. Since the transmission signal through a single PWR spent fuel pin is diminished by approximately 75% (scattering and absorption losses), the number of neutrons per energy bin is then further reduced to 1.17 n s^{-1} bin^{-1}. Assuming a neutron detector efficiency of 20% in this energy range, the final number of neutrons per energy bin is then estimated to be 0.234 counts s^{-1} bin^{-1}.

Since resonance peaks are approximately 0.5-eV wide, we will have 10 bins per peak using the 0.05-eV wide bins. A reasonable goal is to get 10,000 counts per resonance transmission depression, or 1500 counts per bin. The question now is how long do we need to count to get this many total counts? If we divide the desired number of counts per bin by the count rate per bin, or 1500 ÷ 0.234 = 6,410 seconds = 106

minutes = 1.78 hours. For an 8-pin row assay, the neutron attenuation through the 8 pins leads is approximately at 10% transmission reduction in the neutrons, as opposed to the 75% through a single pin. Therefore, for the 8-pin assay, the count time goes up to 13.4 hours. For a single detector this is likely too long for a safeguards-relevant measurement. However, if multiple detectors are used to allow complete assay of multiple sections of an assembly simultaneously, this may be acceptable.

In order to achieve shorter-duration count times a higher-intensity neutron source would be needed. If we desire to reduce the 8-pin count time from 13.4 hours to approximately 20 minutes, the neutron source strength would need to be increased by a factor of 40. A factor of 40 would increase the neutron source strength to approximately 1.1×10^{13} n/s; count times will be decreased to 2.65 minutes for a single pin and 20.1 minutes for the 8-pin row assays, respectively.

There are a several ways to get this factor of 40 increase in the neutron intensity, considering modifications to the base-line Auditore–type neutron source. These include a) increasing the accelerator electron energy, b) increasing the average beam current, c) changing out the tungsten converter for a depleted uranium converter, and c) optimizing the beryllium converter dimensions. Therefore, small adjustments to several system parameters should allow us to readily achieve the desired factor of 40. For example, we can increase the electron energy from 10 to 30 MeV and get a factor of 8 to 10 improvement (Figure 4). Increasing the beam current from 100 to 200 μA gets another factor of 2. Replacing the tungsten with depleted uranium will get another factor of 2, and optimizing the dimensions of the beryllium for the higher energy while optimizing the depleted uranium thickness should get another factor of 2. The combined product would be a factor of approximately 40, achieving the yield improvement and the reduction in count times.

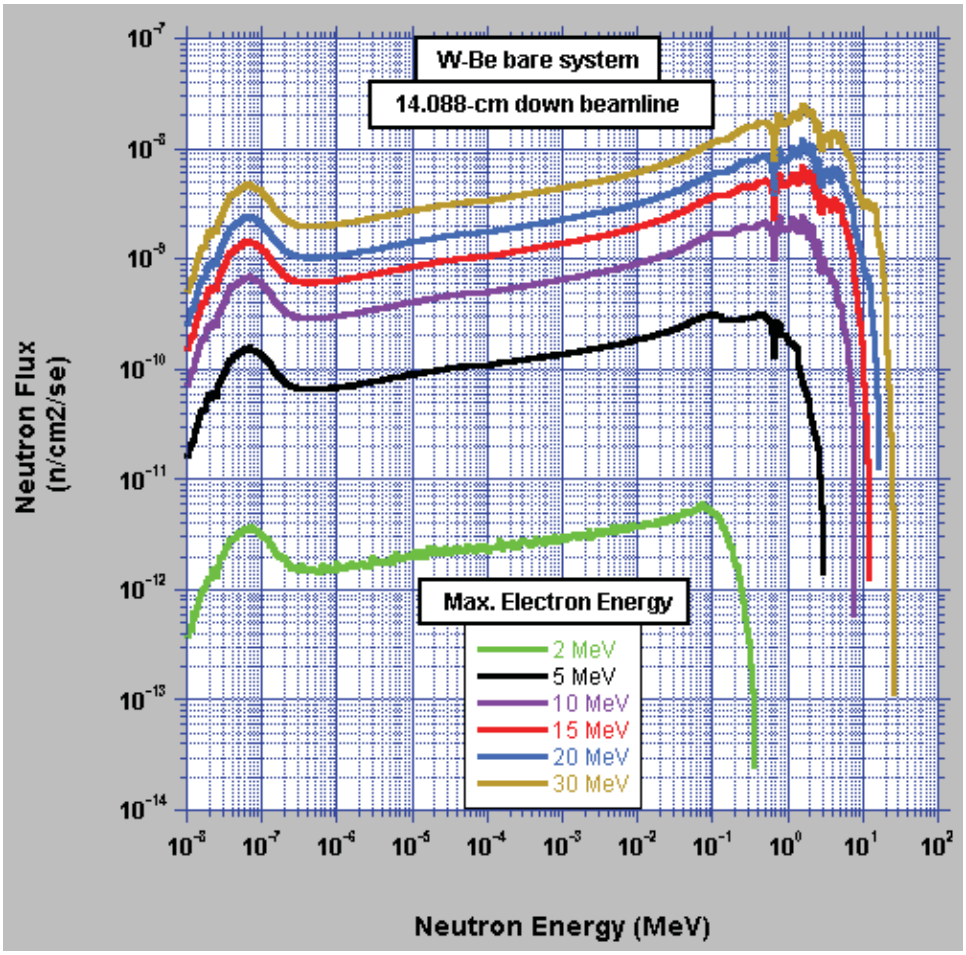

Figure 4 Calculated neutron flux spectra per unit of beam current down the beam line exiting end of the beryllium converter. (Purple line is 10 MeV, from 10 to 30 MeV produces a factor of approximately 10 in neutron intensity).

It should be noted that spent fuel emits both spontaneous fission neutrons and (alpha,n) neutrons which together can produce a neutron background. In reference [2] it was shown for the NRTA system that with appropriate neutron shielding around the evacuated flight tube aft of the chamber holding the spent fuel assembly or between the spent fuel assembly and the neutron detectors, and assuming at least a 3-m long section of flight tube between the spent fuel assembly and the neutron detectors, the neutron background signal would be negligible.

4.3 Temperature Effect

Radioactive materials in a spent nuclear fuel assembly will generate heat with the possibility of increasing the fuel temperature, especially if the assembly is suspended in air as is required for the NRTA assay technique. Increased fuel temperature will Doppler-broaden neutron resonances and potentially affect the NRTA transmission signal This section attempts to quantify the magnitude of this effect through the presentation of calculated transmission spectra for a single PWR fuel pin at five different temperatures.

In our conceptual design for the NRTA technique a spent fuel assembly undergoing an assay will be placed in an air-filled column where the assembly can be raised and lowered, rotated about its vertical axis, and moved transversely. The assembly, which generates heat primarily through fission product decay processes, will be cooled by forced-air convection. The air flow rate through the tube needed to maintain an acceptable fuel/clad temperature is not yet known; the amount of cooling being dependent on the assembly burnup, cooling time, and structural integrity limits. An acceptable temperature for the fuel assembly should probably be restricted to 100-300 ºC, likely closer to 100 ºC.

An increase in fuel temperature results in the Doppler-broadening of heavy nuclide resonances. For the NRTA technique this translates directly into a broadening of the transmission resonance depressions. The depth of the depressions (or dips) is reduced and the width expanded or broadened in energy. The reduction in the depth of the signal depression can directly affect the plutonium estimate depending on the method used to estimate the plutonium mass.

This conceptual study attempts to determine how much of an effect the fuel temperature has on the calculated transmission signal and in particular if the effect is significant over the 100-300 ºC temperature range. In order to evaluate this temperature effect, a single PWR fuel pin with a 15 GWD/MTU burnup, initial 3 wt% enrichment, and a one-year cooling time was modeled using specially generated ENDF-7 temperature-dependent cross sections for the actinides and fission products in the MCNP model. Although burnup and cooling time would normally be the determining factors for amount of cooling required to maintain an acceptable fuel temperature, the calculations here simply assume elevated fuel temperatures using appropriately Doppler-broadened neutron cross sections.

Figure 5 shows calculated transmission spectra for five different fuel temperatures (20, 327, 627, 927, and 2226 ºC). Over the 0-40 eV range in this figure, one can see slight coloration effects due to the different fuel temperatures. Detailed differences in the transmission spectra are more easily visualized in expanded scale (Figure 6).

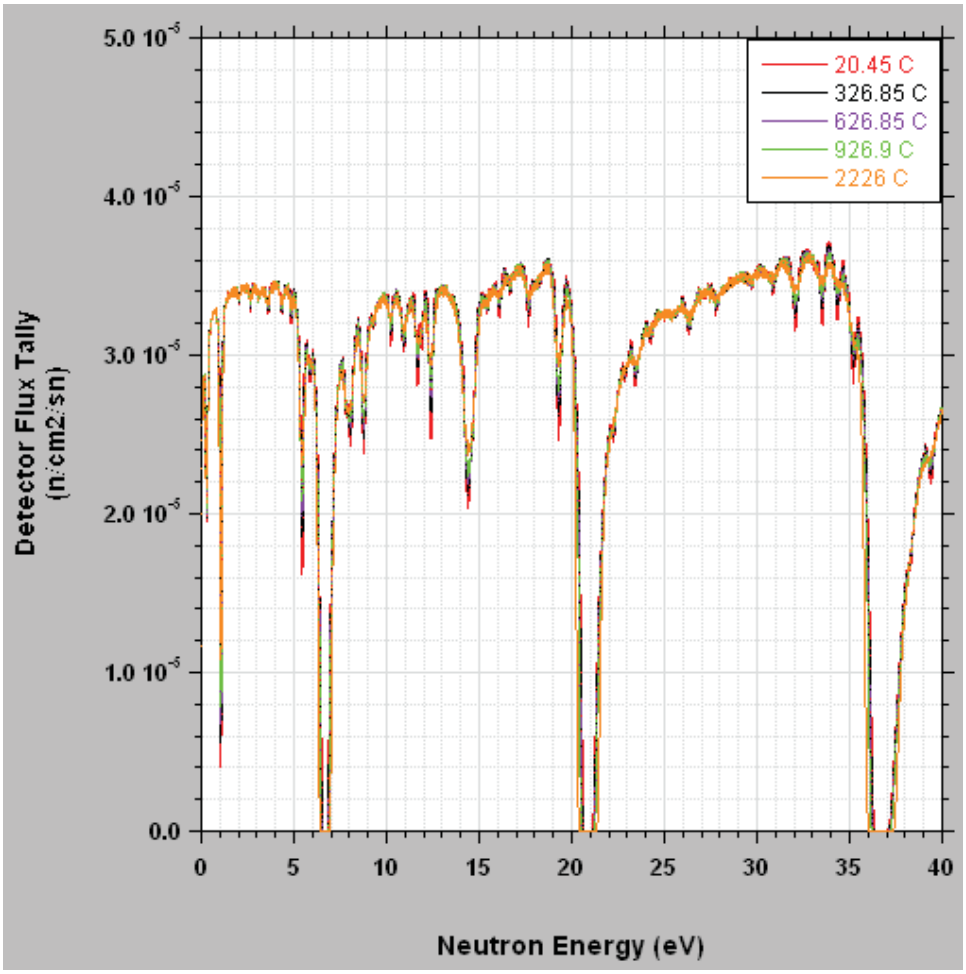

Figure 5 Calculated temperature-dependent transmission spectra through a single spent fuel PWR fuel pin.

Figure 6 is an expanded view of the calculated spectra; zoomed-in to show just the ^{240}Pu resonance at 1.06 eV. Here the effects of Doppler-broadening are self-evident; the resonance depression depth decreases with increasing temperature and the resonance wings broaden in a corresponding manner so as to preserve the overall area of the depression.

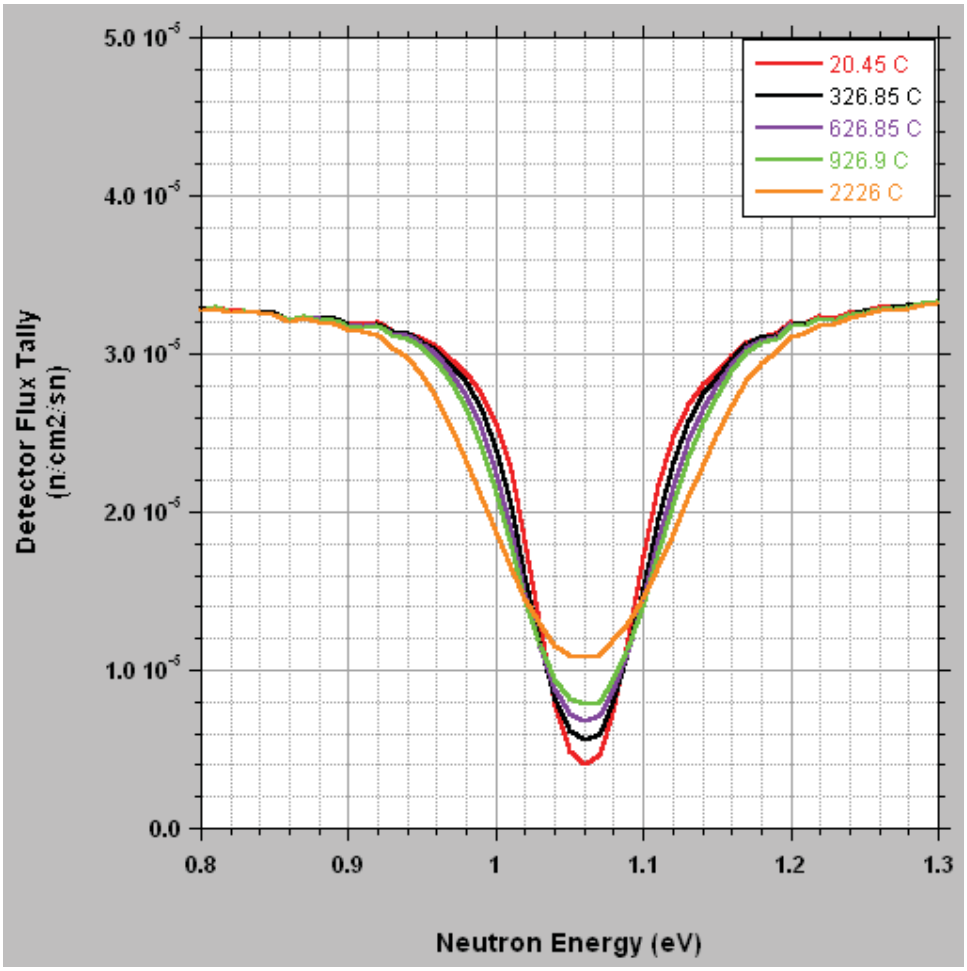

Figure 6 Expanded view of the Doppler-broadened Pu-240 resonance depression at 1.06 eV.

A jump in fuel temperature from room temperature (20.45 ºC) to 326.85 ºC results in an approximately 7.0% decrease in depth of the ^{240}Pu resonance. This is a significant change in the resonance depth and could affect the plutonium mass estimate for the PWR assembly using the maximum depression depth to estimate plutonium mass.

Fortunately the temperature effect here can be mitigated via several possibilities: (1) the forced air-convection cooling could be increased so as to maintain the assembly temperature below a temperature such that Doppler-broadening is not a concern, for example, <150 ºC, (2) use of a temperature measuring device to estimate the fuel temperature and correct the measured transmission spectrum for Doppler-broadening, and (3) use of full-peak time-spectra analyses, the "area method," to estimate plutonium mass versus simple peak-depression (peak height) analysis, since the area "above" the depression is constant regardless of fuel temperature (the area under a neutron resonance is constant at any fuel temperature). Therefore, despite the fact that decay heat will tend to increase the fuel temperature while the assembly is suspended in air during

transmission measurements, the temperature increase can be limited with forced air-convection cooling and an "area method" utilized to estimate plutonium mass. Hence, assembly fuel temperature is no longer a significant issue for NRTA.

4.4 Plutonium-239 Assembly Mass Estimate

The concept studies demonstrated that four uranium isotopes (^{234}U, ^{235}U, ^{236}U, ^{238}U), four plutonium isotopes (^{239}Pu, ^{240}Pu, ^{241}Pu, ^{242}Pu), two americium isotopes (^{241}Am, ^{243}Am), and six fission product isotopes (^{99}Tc, ^{103}Rh, ^{131}Xe, ^{133}Cs, ^{145}Nd, ^{152}Sm) could be readily identified in the calculated spent fuel transmission spectra. Theoretically, given a measured transmission spectra, a mass estimate for each and every one of these isotopes could be derived from the transmission spectra. Interestingly, it would require only one resonance per isotope to derive this mass estimate. Since most actinide isotopes have multiple resonances in the 0-20 eV range, mass estimates derived from multiple resonances could provide isotopic mass confirmation or a basis for an average value. It should also be noted that the single resonance chosen for the mass estimate need not necessarily be well-isolated or totally free of other-resonance interference.

The method we shall employ to derive a mass estimate from the transmission spectra will be referred to here as the "depth" method, details of which are described below for the application demonstration. The "depth" method simply measures the depth of the resonance depression in the transmission spectra (this is a simpler analytical approach than the "area method" described in the previous section). A straight line is drawn over the top of the depression from the high points on each side of the depression and then the attenuation from the point on the line corresponding to the resonant energy to the bottom of the depression is measured and recorded as the "a" value, in counts. The other important length to be measured is the distance from the bottom of the depression to zero on the ordinate axis (number of detector counts). The transmission factor (T) is then the ratio of "b" divided by "a+b;" using this transmission factor (T), the mass can be derived.

Unfortunately, the "depth" method relies strongly on selecting a resonance that is well-isolated and does not have significant interference from other resonances. Although measured transmission spectra appear to have well-defined resonance structure, the 0-20 eV energy range contains a multitude of isotopic resonances and each resonance is undoubtedly affected by resonance interference to some degree. As a further complication, it is also expected that there are small and narrow or just narrow actinide and fission product resonances hidden beneath each of the well-defined visible resonances in the measured transmission spectra. These problems can be solved through more sophisticated analysis tools that can unfold the spectra and provide a "corrected" resonance depression for the "depth" method analysis.

For demonstration purposes, in our mass estimate below we have chosen to only evaluate ^{239}Pu. We could have chosen any or all of the identified isotopes in the transmission spectra, however due to time constraints and our limited goal to demonstrate the simplicity of the mass estimation process associated with the NRTA technique, we chose just the one isotope. In addition, although there are multiple ^{239}Pu resonances, we

chose just the 10.93-eV ^{239}Pu resonance for the evaluation. This particular resonance appears to be relatively well isolated; however, resonance interference still affect this mass estimate.

Since we lack actual test data, calculated transmission spectra are used in place of actual measured data. Theoretically, one should expect to derive the exact ^{239}Pu mass as used in the MCNP model. This however is not the case. Resonance overlap and potentially hidden resonances within the 10.93-eV resonance skew the transmission factor (T) that is estimated from the plotted calculated transmission spectra. Since we do not currently have the analytical tools needed to unfold the spectra and correct the resonance depression, the mass estimates are going to be off by the degree of resonance interference. For fresh fuel with only ^{235}U and ^{238}U, the calculated transmission spectra or resonance depressions one would expect have much less resonance interference. For example, an isolated ^{235}U resonance could be chosen such that the ^{235}U mass could be estimated from the calculated transmission spectra to better than 1% relative to the actual ^{235}U mass (number density) used in the MCNP transmission model. For spent fuel, the analysis presented here demonstrates that more sophisticated transmission analysis tools will be required to unfold the resonance depressions in the transmission spectra in order to achieve a higher degree of accuracy for isotopic mass estimates.

For the ^{239}Pu estimate, we will use a PWR spent fuel assembly with a burnup of 45 GWD/MTU, initial enrichment of 3 wt% ^{235}U, and a 1-year cooling time. The fuel composition is taken directly from LANL spent fuel library #1, where each of the 264 fuel pins in the assembly has been divided into four annular radial fuel depletion regions with a single axial region over the full fuel pin length. The depleted fuel assembly has 39 different depleted fuel pins and a total of 156 different fuel compositions. In LANL library #1, the fuel assembly has depleted fuel pin symmetry about the horizontal and vertical axes through the center of the assembly, as well as symmetry about the two diagonal axes through the corners and center of the assembly. The assumed quadrant symmetry for the depletion regions in the fuel assembly requires only 39 different depleted fuel pins in the entire assembly.

Table 2 and Table 3 give the actinide isotopic total mass distribution for the 45 GWD/MTU spent PWR fuel assembly and the ^{239}Pu mass (grams) per fuel pin composition (1-39), respectively. Figure 7 shows the distribution of the fuel pin composition numbers (1-39) across the PWR assembly. Note that the number “50” is a control rod guide tube location and not a fuel pin; “39” is a corner pin, for example. These data are used in the MCNP transmission models used to calculate the transmission spectra.

Table 2 Actinide isotopic total mass distribution for the 45 GWD/MTU spent PWR fuel assembly.

Isotope	Mass [g]	Isotope	Mass [g]
U-233	0.00	Pu-244	0.03
U-234	2.38	Am-241	59.45
U-235	1,905.82	Am-242	0.14
U-236	1,943.01	Am-243	113.83
U-238	445,657.04	Cm-242	2.77
Np-238	0.00	Cm-243	0.37
Np-237	272.80	Cm-244	70.78
Pu-238	137.18	Cm-245	5.40
Pu-239	2,610.45	Cm-246	0.80
Pu-240	1,338.49	Cm-247	0.01
Pu-241	769.38	Cm-248	0.00
Pu-242	479.04		

Table 3 The ^{239}Pu mass in each fuel pin.

Pin No.	Mass [g]	Pin No.	Mass [g]	Pin No.	Mass [g]	Pin No.	Mass [g]
1	9.36278	11	9.62499	21	10.14340	31	9.88143
2	9.37585	12	9.70237	22	9.42148	32	10.25770
3	9.41015	13	9.93914	23	9.47961	33	10.47010
4	9.63298	14	10.20360	24	9.91120	34	10.23820
5	9.85900	15	9.46053	25	10.14270	35	10.48930
6	10.10500	16	9.43939	26	9.51392	36	10.64330
7	9.48391	17	9.51726	27	9.54918	37	10.67390
8	9.50585	18	9.56721	28	9.70351	38	10.80740
9	9.39555	19	9.63111	29	10.07550	39	10.86020
10	9.56791	20	9.98960	30	10.25720		

39	38	36	33	30	25	21	14	6	14	21	25	30	33	36	38	39
38	37	35	32	29	24	20	13	5	13	20	24	29	32	35	37	38
36	35	34	31	28	50	19	12	50	12	19	50	28	31	34	35	36
33	32	31	50	27	23	18	11	4	11	18	23	27	50	31	32	33
30	29	28	27	26	22	17	10	3	10	17	22	26	27	28	29	30
25	24	50	23	22	50	16	9	50	9	16	50	22	23	50	24	25
21	20	19	18	17	16	15	8	2	8	15	16	17	18	19	20	21
14	13	12	11	10	9	8	7	1	7	8	9	10	11	12	13	14
6	5	50	4	3	50	2	1	50	1	2	50	3	4	50	5	6
14	13	12	11	10	9	8	7	1	7	8	9	10	11	12	13	14
21	20	19	18	17	16	15	8	2	8	15	16	17	18	19	20	21
25	24	50	23	22	50	16	9	50	9	16	50	22	23	50	24	25
30	29	28	27	26	22	17	10	3	10	17	22	26	27	28	29	30
33	32	31	50	27	23	18	11	4	11	18	23	27	50	31	32	33
36	35	34	31	28	50	19	12	50	12	19	50	28	31	34	35	36
38	37	35	32	29	24	20	13	5	13	20	24	29	32	35	37	38
39	38	36	33	30	25	21	14	6	14	21	25	30	33	36	38	39

Figure 7 The 39 depleted fuel pin numbers and assignment to each location in the 17 × 17 PWR assembly. Note: the number "50" is a control rod guide tube, numbers 1-39 are depleted fuel pin numbers.

From Table 2, the total ^{239}Pu mass in the assembly (45 GWD/MTU) is 2610.45 grams. This is the goal quantity we will attempt to achieve in our ^{239}Pu estimate. Theoretically, in an ideal situation, our ^{239}Pu estimate should equal exactly this value. However, in addition to the resonance overlap problem cited above, there are additional approximations and uncertainties associated with the estimate. It is interesting to note that some of these calculational approximations have a corresponding analog in actual measured transmission spectra. For example, the calculated spectra are actually counts in finite width energy bins which would be similar to the measured spectra where counts are grouped in time bins. Energy bins and time bins determine the signal resolution. The counts in these bins also have an uncertainty; in the Monte Carlo calculation the energy bins an inherent statistical error, and the measurement the time bins have a statistical counting error. Curve-fitting these transmission depression signals would improve the

ability to predict the transmission coefficient but this would require an additional development effort beyond this project, as would the development of additional analytical tools to further evaluate the transmission data. For our purposes here we will visually inspect the plotted transmission data and estimate the transmission factor (T).

For LANL library #1, the ^{239}Pu distribution in the 45 GWD/MTU PWR assembly is highest in the peripheral fuel pins and decreases towards the center of the assembly. The interior pins are relatively uniform in ^{239}Pu mass and, for an 8-pin assay, we take advantage of this interior uniformity for the total assembly ^{239}Pu mass estimate. A good example of the ^{239}Pu uniformity is shown in Figure 8.[27] Even though this particular assembly had an asymmetrical burnup history, the interior fuel pins exhibit a relatively uniform ^{239}Pu distribution.

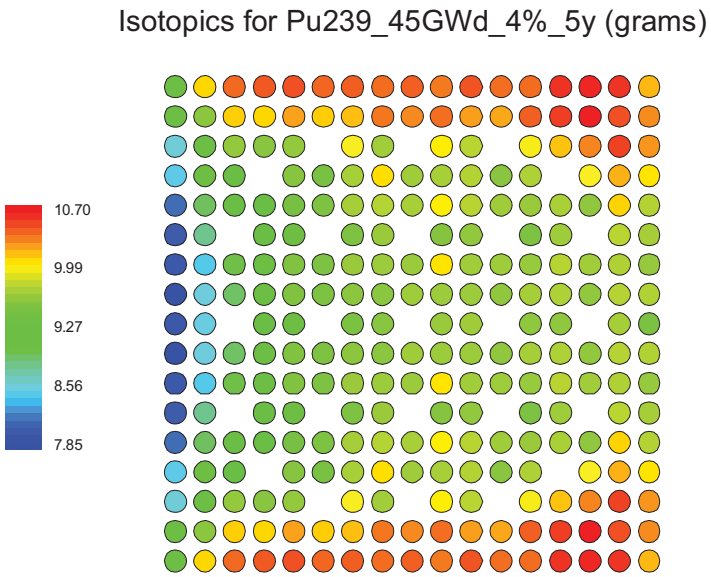

Figure 8 Mass distribution for ^{239}Pu (grams) per pin from LANL spent fuel library #2 with 4 wt% initial enrichment and a burnup of 45 GWD/MTU.[27]

For an ^{239}Pu estimate, we also assume that the fuel pins are perfectly aligned with no bowing. This assumption is not critical in the calculation nor is it critical in an actual NRTA measurement as long as the detector can spatially resolve the fuel pin and the gap space between the pins. (If individual fuel pin assay is not needed then bowing is irrelevant). In our transmission calculation spatial increments of 0.1 cm across the fuel pin are used and result in five transmission spectra across the fuel pin diameter starting at the pin center. Figure 9 shows the five transmission paths with 0.1 cm widths used in the transmission calculations. The five transmission paths are numbered as follows: 0.0-0.1 cm (dX.1), 0.1-0.2 cm (dX.2), 0.2-0.3 cm (dX.3), 0.3-0.4 cm (dX.4), and 0.4-0.5 cm (dX.5), where X is the scan number (1-15). The fifth or outer path (0.4-0.5 cm width) intersects only a tiny outer peripheral region of the UO_2 fuel and its transmission spectrum is virtually flat and contributes very little to the overall assay.

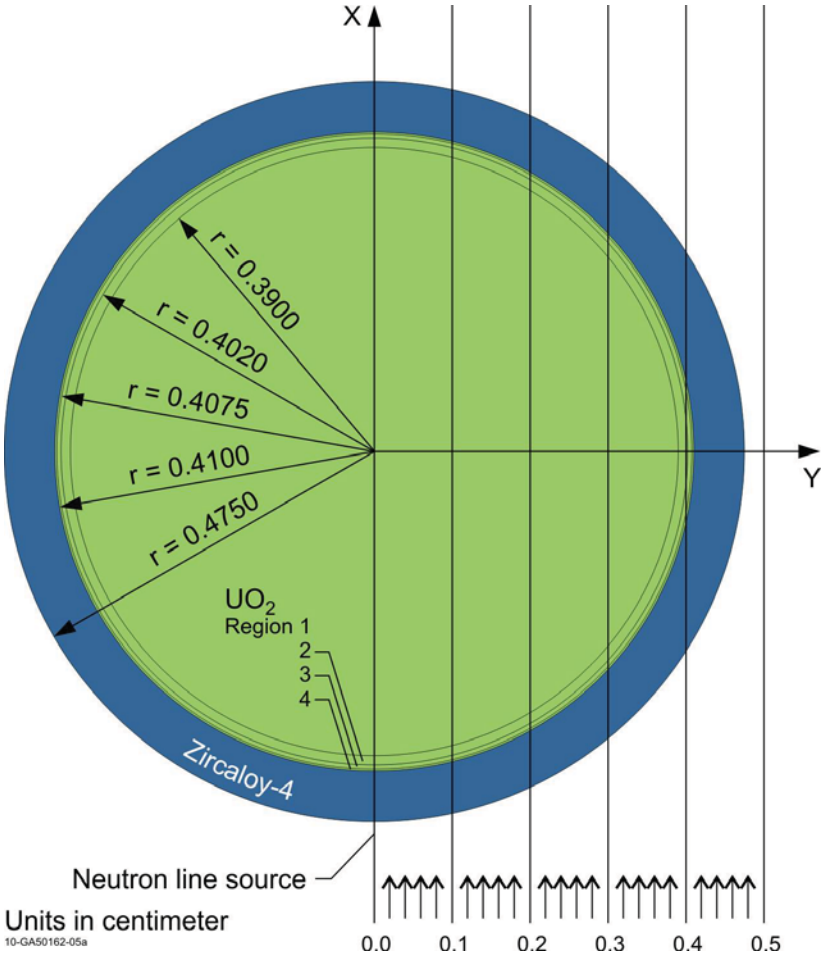

Figure 9 Transmission swaths through the fuel pin(s).

An additional assumption is that the ^{239}Pu mass distribution is uniform over the full length (0.366 m) of the fuel pin. Although there is some axial variation in the ^{239}Pu distribution in an actual PWR fuel pin, it is relatively uniform except near the extreme ends of the fuel pin. The NRTA technique could take multiple scans at different axial locations along the fuel pin as mentioned in the section on "Multiplexing".

Figure 10 shows an example for calculating a transmission spectrum and how the "depth" method is used to determine the transmission factor T. The plotted transmission spectrum shown is for the 8-14 eV portion of the energy spectrum which included the ^{239}Pu resonance depression of interest at 10.93 eV. The red-hatched area is the transmission depression due to the ^{239}Pu 10.93 eV resonance. The lengths "a" and "b" are shown and estimated by simply drawing a straight line (red) across the top of the depression and measuring the "a" and "b" distances. The transmission factor T is then given by the formula: T = b/(a+b).

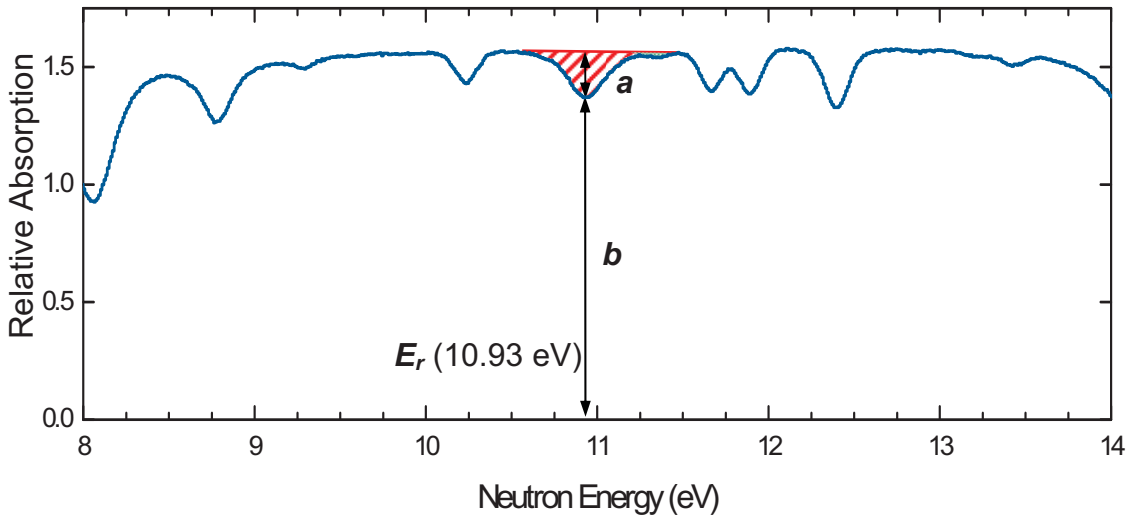

Figure 10 Estimation of the transmission factor (T) using the 10.93 eV resonance depression from ^{239}Pu. The transmission factor T is simply given by T = b/(a+b).

The transmission factor (T) is related to the average ^{239}Pu number density (N) in the transmission path by the following attenuation formula:

$$T(E_r) = \frac{b}{a+b} = e^{-N\,\sigma(E_r)\,x} \qquad \text{Eq. 2}$$

where $T(E_r)$ is the transmission factor at the resonant energy, σ is the magnitude of the ^{239}Pu total cross section at the resonant energy (10.93 eV), and x the average chord length of the transmission path through the fuel pin(s) in an assay row. A brief description of the calculational procedure used for estimating the ^{239}Pu mass for a given transmission spectra follows.

First, a transmission spectrum is calculated for a particular scan or a fixed number of pins in a row; five different spectra per scan. For complete coverage of the PWR assembly (every pin included in at least one scan), 16 different scans (d1-d16) are needed (Figure 11). Most of the scans are diagonal scans starting with the corner pin (1-pin scan) in the lower right-hand corner of the PWR assembly. This is the "d1" line shown in Figure 11 for the single corner pin. The other 15 pin row scans are also shown in Figure 11 as d2—d16. The 16 scans include 14 of the 17 diagonal rows starting with the corner pin (d1) plus two non-diagonal scans which are vertical rows with 12 pins each (d10 and d16). Note that three of the possible diagonal rows of pins were excluded, because these rows of pins exceeded 12 pins; these three rows of pins have 13, 15, and 16 pins. All the other vertical rows besides d10 and d16 have more than 12 pins per row as well. The control rod guide tubes are the larger white circles.

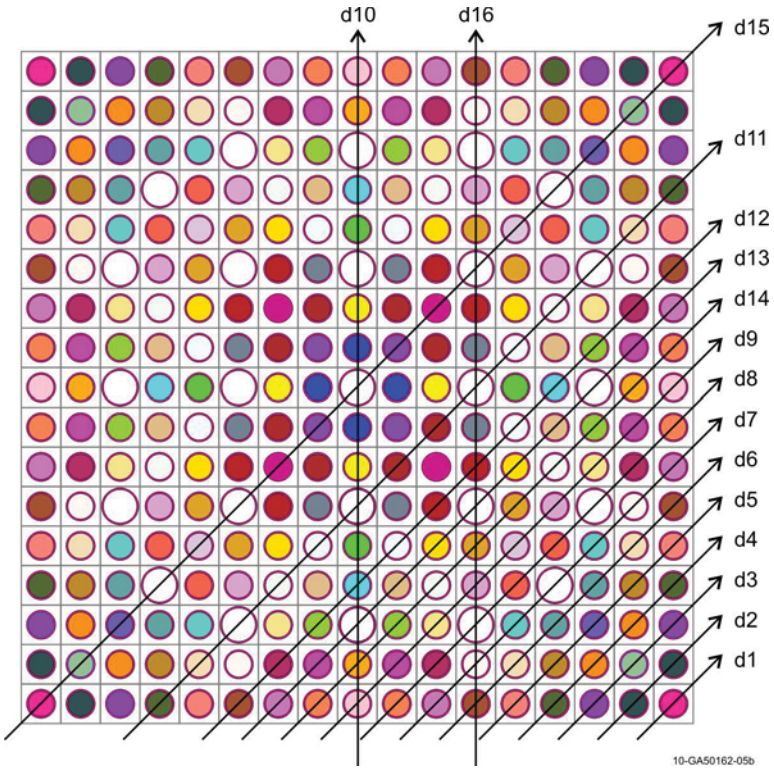

Figure 11 The 15 pin rows (d1-d15) used in the transmission spectra calculations.

Figure 12 shows five typical calculated transmission spectra for a given scan. In this case, the transmission spectra are for the d6 transmission scan. The d6-scan is through the 6-pin row with pins 25-29-31-31-29-25. The blue curve (d6.1) of Figure 12 is through the thickest part of the fuel pin (0.0-0.1 cm), the green curve (d6.2) is through 0.1-0.2 cm, the gold curve (d6.3) is through 0.2-0.3 cm, the purple curve (d6.4) is through 0.3-0.4, and the red curve (d6.5) is through 0.4-0.5 cm. The UO_2 pellet radius is only 0.41 cm; hence the fifth or red curve exhibits little attenuation.

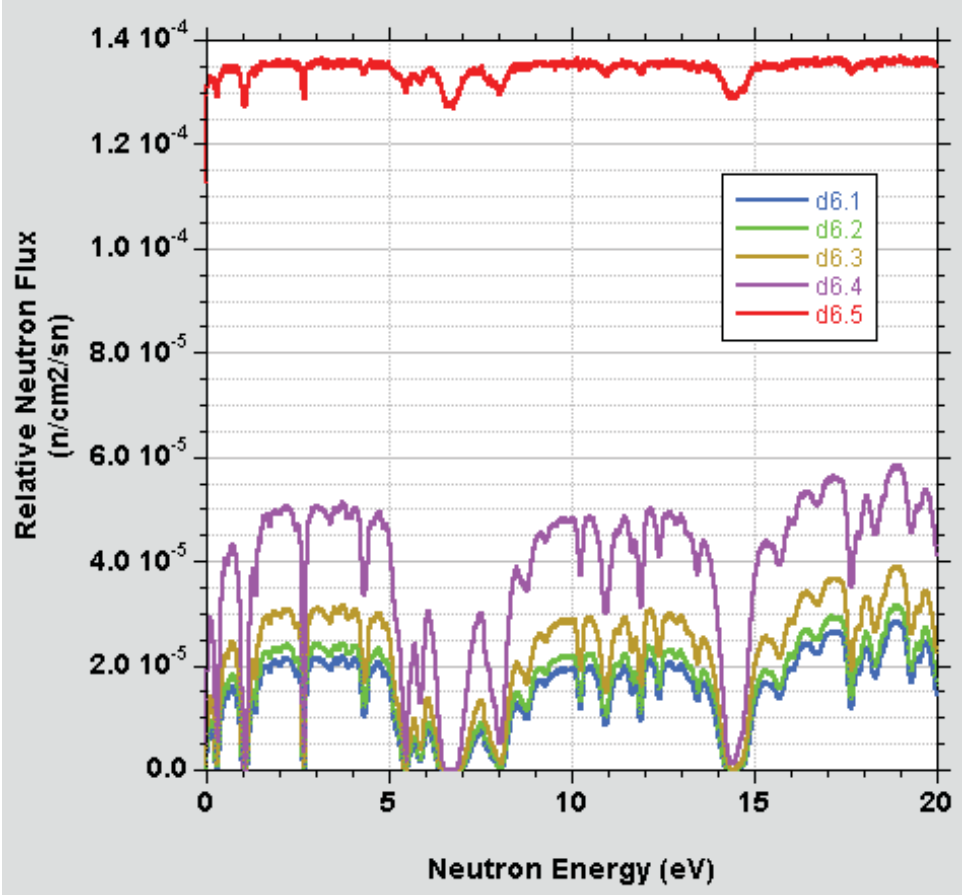

Figure 12 Typical calculated transmission curves for the d6-scan.

Figure 13 is the same as Figure 12 but expanded to just the 10-12 eV energy range encompassing the 10.93 eV ^{239}Pu resonance depression. The figure designations d6.1 and d6.4, for example, correspond to the d6 transmission and the ".1" and ".4" correspond to the transmission paths widths of 0.0-0.1 and 0.3-0.4 cm, respectively, as shown above. Note the increased signal attenuation for the greater average chord length (x) of material traversed by the transmission neutrons: d6.1<d6.2<d6.3<d6.4.

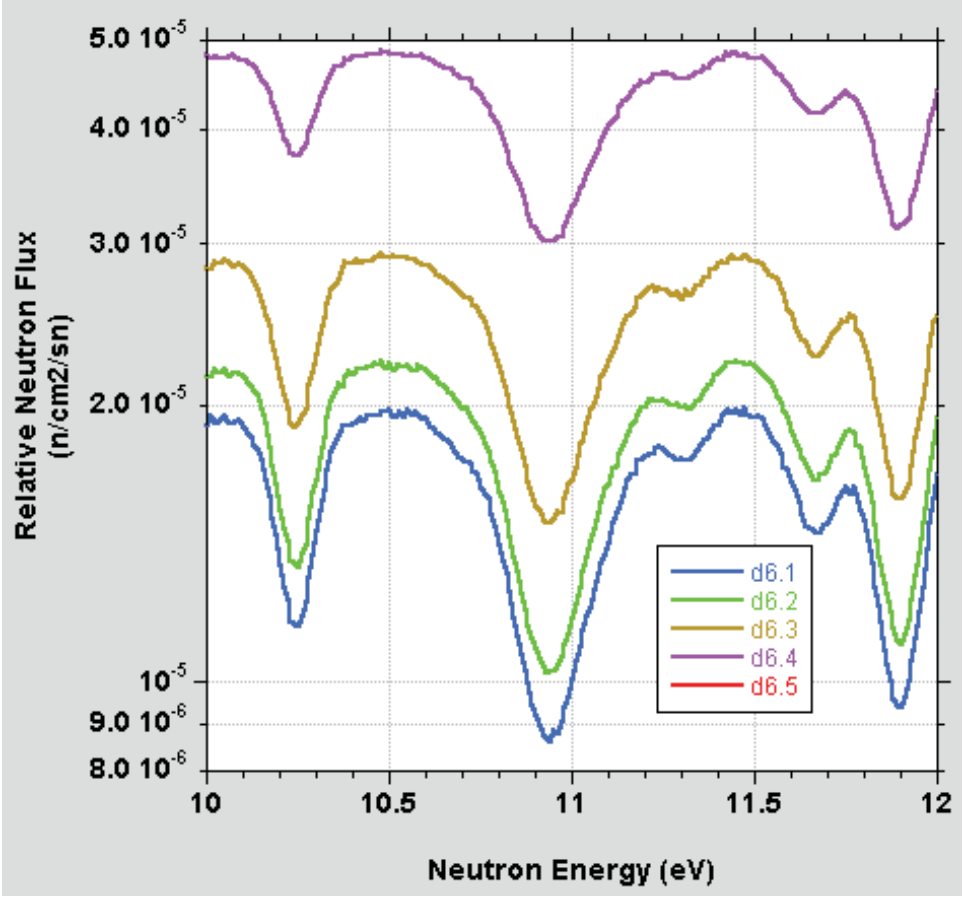

Figure 13 Typical calculated transmission curves for the d6-scan expanded to show the ^{239}Pu 10.93 eV resonance used to estimate the transmission factor, T.

Applying the "depth" method to the calculated transmission curves, it was straightforward to estimate the ^{239}Pu mass in 15 of the 16 scans (d1-d15). The sixteenth scan (d16) was omitted in the calculations here due to time constraints at the end of the fiscal year. Table 4 gives the calculated mass estimate (Calc. Mass) in grams along with the mass from the LANL library fuel compositions (Lib. Mass) for scan numbers d1 through d15. The last column is the percent difference between the calculated mass and the LANL library mass. The percent difference, calculated as 100 * (Calc. Mass - Lib. Mass)/(Lib. Mass), is always negative which means the calculated mass always under predicts the library values and tends to increase in negative magnitude with increasing number of fuel pins per row. The under prediction is believed to be the direct result of resonance overlap (resonance interference) which the simplistic peak-height analysis method is susceptible to. It is also possible that small fission product or actinide resonances may be present inside the ^{239}Pu 10.93-eV resonance but a search for these has not yet been performed. The net result of resonance interferences is the increased absorption or out-scatter of transmission neutrons, which changes in the "a" and "b" lengths in the attenuation formula such that a smaller mass of ^{239}Pu is always estimated.

Table 4 Results of the ^{239}Pu estimate by scan row.

Scan No.	No. of Pins	Fuel Pins in Each Scan	Lib. Mass [g]	Calc. Mass [g]	Diff. [%]
d1	1	39	10.86	10.49	-3.4
d2	2	38-38	21.62	20.82	-3.7
d3	3	36-37-36	31.96	30.51	-4.5
d4	4	33-35-35-33	41.92	41.04	-2.1
d5	5	30-32-34-32-30	51.27	48.61	-5.2
d6	6	25-29-31-31-29-25	60.20	57.40	-4.7
d7	6	21-24-28-28-24-21	59.52	57.41	-3.5
d8	6	14-20-27-27-20-14	59.48	57.29	-3.7
d9	9	6-13-19-23-26-23-19-13-6	87.82	83.02	-5.5
d10	12	6-5-4-3-2-1-1-2-3-4-5-6	115.49	103.55	-10.3
d11	10	33-29-18-10-8-8-10-18-29-33	98.37	89.04	-9.5
d12	12	25-20-12-4-10-16-16-10-4-12-20-25	116.95	105.75	-9.6
d13	8	21-13-11-17-17-11-13-21	78.45	73.75	-6.0
d14	10	14-5-12-18-22-22-18-12-5-14	97.51	89.42	-8.3
d15	12	39-37-34-26-15-7-7-15-26-34-37-39	120.46	110.51	-8.3
d16	12	25-24-23-22-16-9-9-16-22-23-24-25	---	---	---

The calculated transmission spectra can now be used to develop estimates of the total ^{239}Pu mass in the assembly. Under the assumptions stated above, and limiting the discussion to a set of scans only reaching a total thickness of 8-pins in a row (the d1-d8 and d13 scans, which may be the practical limit for attenuation assays), the total ^{239}Pu assembly mass is estimated to be 2,511 grams. Compared to the actual total ^{239}Pu assembly mass of 2,610.45 grams, this is a difference of -3.80%. For the estimate, the bulk of the interior pins which, those not included in the d1-d8, d13 scans, were set equal to the average ^{239}Pu mass per pin from the d13 scan. The -3.80% difference is directly attributable to resonance interferences. It is likely this can be improved upon using more sophisticated assay analysis techniques beyond the 'peak height' analysis used here.

If we assume now that NRTA can measure up to 12-pins per row, then all 15 scans (d1-d15) can be used in the total ^{239}Pu assembly estimate. The total ^{239}Pu assembly mass is then estimated to be 2,488 grams. Compared to the actual total ^{239}Pu assembly mass of 2,610.45 grams, this is now a -4.68% difference. The difference is due again to resonance interference but is also impacted by some signal degradation due to the notably larger UO_2 distance traversed in the 9-12 pin scans. Note the percent difference in Table 4 tends to increase with the number of pins in a row. The lower total inventory of 2,488 grams is also due to the generally lower average ^{239}Pu pin content of the interior pins relative to peripheral pins, as shown in Table 5.

Table 5 Estimated average ^{239}Pu pin content by transmission scan.

Scan No.	Average ^{239}Pu mass [g]
d1	10.4904
d2	10.4086
d3	10.1711
d4	10.2590
d5	9.7220
d6	9.5674
d7	9.5679
d8	9.5474
d9	9.2249
d10	8.6295
d11	8.9042
d12	8.8123
d13	9.2191
d14	8.9423
d15	9.2090

For the 12-pin scan capability, in particular, an approach would need to be developed to determine how best to allocate the average ^{239}Pu pin mass determined from the 16 integral transmission scans. This appraoch would be used to improve the total ^{239}Pu assembly mass estimate. The NRTA technique with 12-pin scan capability allows for every pin in the assembly to be part of one or more scans. Starting with the corner pins it might be possible to completely determine the ^{239}Pu mass content of each pin in the assembly to a high degree of accuracy. Some approximation may be required for the interior pins, but again the interior pins have a fairly uniform ^{239}Pu distribution and many are included in multiple scans.

Despite the potential need for a larger neutron source strength and perhaps longer count times, an NRTA 12-pin scan capability would be able to quickly detect diversion of any pin in the assembly. Plus, a sophisticated analysis tool to unfold the transmission spectra and correct the spectra for resonance interferences would potentially allow ^{239}Pu mass estimates to approach 1-2% accuracy for the entire assembly. This would also be true for the other plutonium (^{240}Pu, ^{241}Pu, ^{242}Pu), uranium (^{235}U, ^{236}U, ^{238}U), and fission product (^{99}Tc, ^{103}Rh, ^{131}Xe, ^{133}Cs, ^{145}Nd, and ^{152}Sm) isotopes in the assembly. Use of multiple isotopic resonances could be also be used to confirm and/or increase the accuracy of isotopic mass estimates. It is anticipated that different isotopic resonances would be useful at different assembly burnups and cooling times.

4.5 Multiplexing

Use of a high-power, accelerator-based neutron source may be perceived as a significant drawback of the NRTA technique. However, it may be possible to take advantage of the isotropic nature of this type of neurons source to permit the simultaneous analysis of multiple fuel assemblies. The first concept for analyzing an

assembly would be to scan one section of the fuel, and then rotate it to get the orthogonal views. This would achieve the multiple views needed to assay an assembly at one elevation. However, if it was required to assay the complete assembly top-to-bottom this approach would be time consuming. An alternate approach would be to simultaneously collect data at multiple elevations on the assembly at the same time. A comparison of these two approaches is presented in Figure 14. Secondly, whether using one detector or multiple detectors, the simplest approach would be to scan a single assembly at a time. However, the isotropic neutron sources proposed for NRTA would all permit measuring multiple assemblies in parallel, as illustrated in Figure 15.

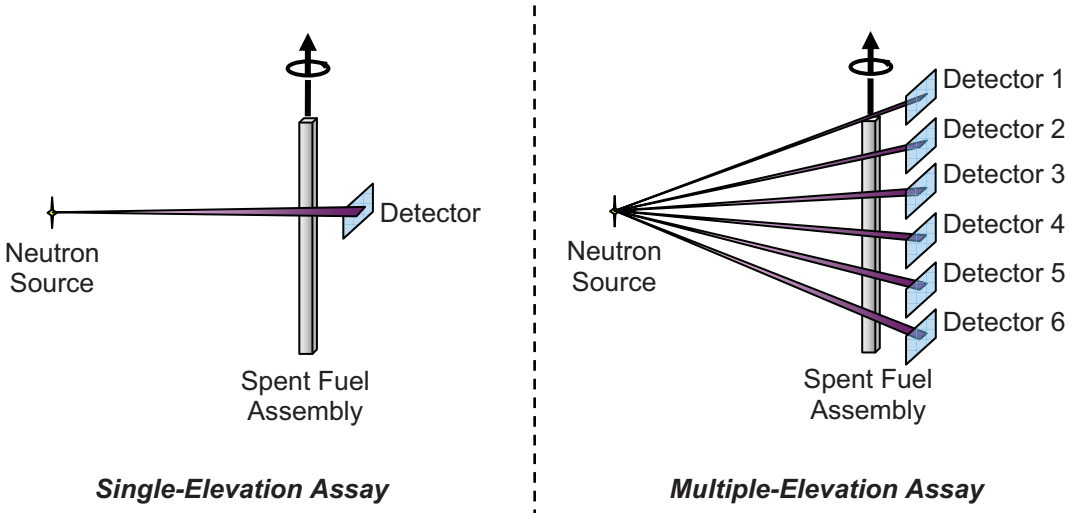

Figure 14 Comparison of the single-elevation assay concept versus a more comprehensive multiple-elevation assay approach.

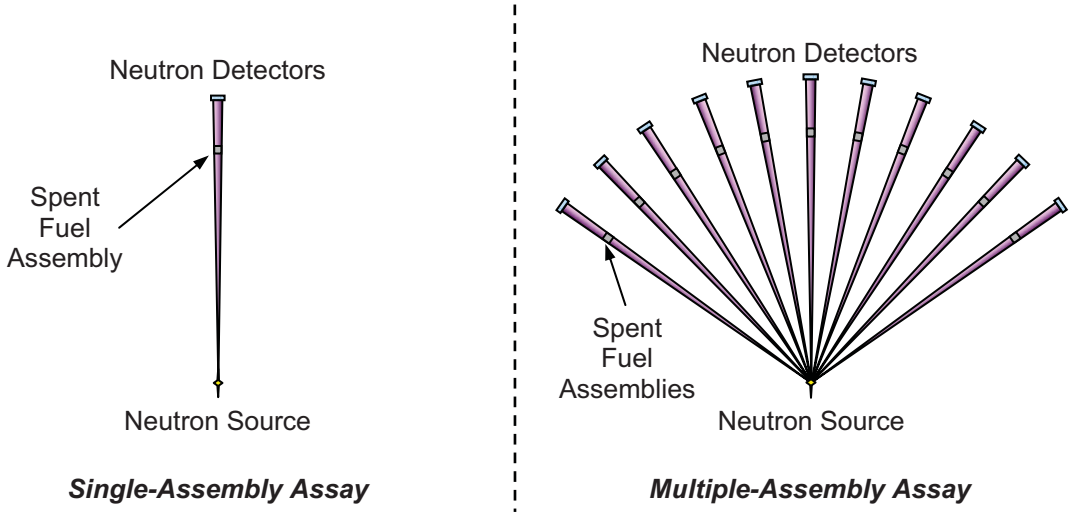

Figure 15 Comparison of the single-assembly assay concept versus a more comprehensive multiple-assembly assay approach.

4.6 Neutron Detectors

Helium-3 detectors based on the $^{3}He(n,p)^{3}H$ reaction, which has a large cross section of approximately 1000 barns at 1.0 eV, are an attractive choice for slow-neutron detection. The original neutron detectors used at the NBS for NRTA studies was a position-sensing proportional counter (PSPC) that used helium-3 for neutron detection.[28] A representative image from that 1970's-era imaging technology is presented in Figure 16, showing an image of sliver-109 in a braze joint; the image resolution was ~0.5 cm. NBS developed PSPC detectors with a resolution of 0.12 cm for fuel assay measurements. This remains an attractive solution for the NRTA project today for spent fuel assay. Although helium-3 detectors can exhibit some sensitivity to gamma radiation in the form of pulse pileup, leading to potential interferences with neutron pulses, shielding may be used to alleviate this to a degree.

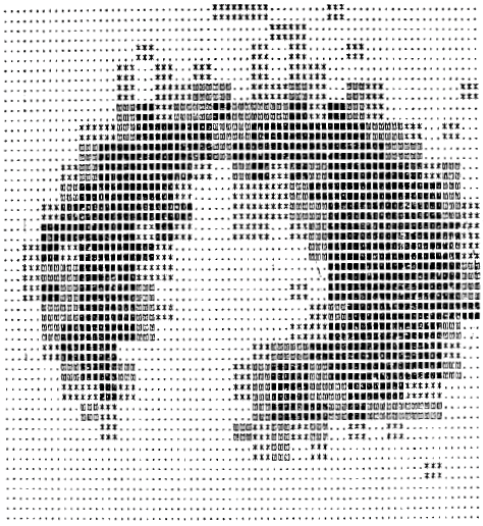

Figure 16 NRTA image of ^{109}Ag in a braze joint of a cylinder, showing incomplete solder flow. The spatial resolution is 0.5 cm.

More recent work, however, shows the significant advances that have been made in real-time, thermal-neutron imagery for NRTA measurements over the past thirty years. In Figure 17 is an example of an NRTA analysis at the KEK laboratory in Japan, which used a gas-electron multiplier (GEM) neutron detector with helium-3.[29] This detector had a spatial resolution <0.5 mm, an image field of view > 30 cm x 30 cm, a detection efficiency > 20%, and could operate with a throughput > 20kcps per pixel. The improved spatial resolution and signal-to-noise performance of this detector is obvious in comparison with the earlier-generation NBS work. While high spatial-resolution imagery isn't necessarily needed for NRTA spent fuel assays it might prove useful for helping to improve local signal-to-noise quality of an assay.

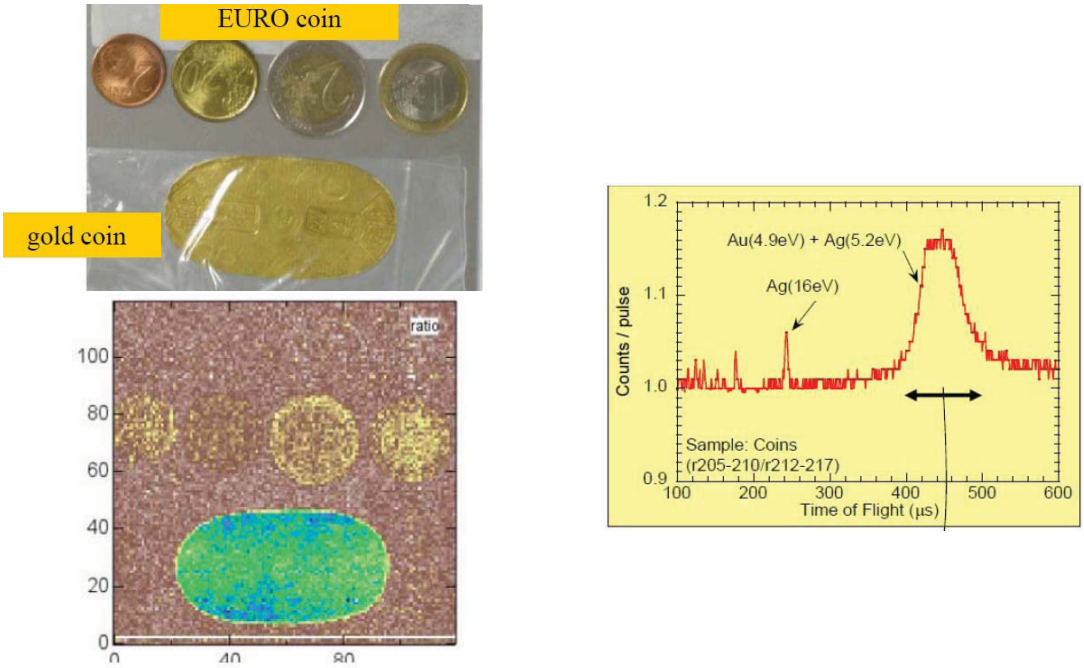

Figure 17 The images on the left show a photograph (top) and NRTA transmission image (bottom) for an assay of silver and gold in European Euro coins. The colors blue and green in the image highlight high concentrations of silver and gold. On the right is an inverse NRTA time spectrum showing the silver and gold resonance features of the image.[29]

Lithium-6 glass scintillator detectors may also prove useful as high-rate count detectors, in particular, a Li-glass scintillator (NE912) enriched to 95% ^{6}Li.[4,9] As a slow-neutron detector the ^{6}Li(n,α)t reaction has a large exothermic Q-value of 4.78 MeV, strong 1/v thermal neutron cross section (approximately 200 barns at 1.0 eV), 7.7% lithium content (NE912), and fast response time. In addition, natural- or depleted-lithium scintillator detectors can be used in conjunction with the enriched detectors to estimate the gamma contribution in a neutron-gamma flux.[6]

5 FUTURE WORK

The fiscal year 2011 tasks have been completed and are documented in this report. Relative to the NGSI NA-241 project, this report represents the final work for the INL NRTA project. The NRTA technique did not make the NGSI down select list for non-destructive techniques, per discussions at the July, 2011, meeting at the 52nd INMM meeting.

Although funding is currently not available to continue NRTA work, several items of interest would be useful to further assess the NRTA technique. In particular, it would be valuable to develop the analytical tools needed to properly evaluate the TOF transmission spectra. Also, we believe a low level of effort activity would be useful for

re-demonstrating some of these measurement principles using an existing NRTA-capable facility.

6 CONCLUSIONS

A preliminary assessment of the nondestructive assay technique known as neutron resonance transmission analysis (NRTA) has been performed by Idaho National Laboratory. There are two parts to the assessment, FY2010 work and FY2011 work. The FY2011 work is documented here and is follow-on or add-on conceptual studies to the FY2010 project. The INL NRTA assessment is not complete (additional assessment work has been identified herein), but preliminary results indicate the NRTA to be a powerful assay technique for spent fuel.

To measure the plutonium mass in a pressurized water reactor spent fuel assembly, it has been estimated that an accelerator-based neutron source with a 4π neutron emission rate would need to have a strength of approximately 8×10^{12} to 1×10^{13} n s^{-1}. This source strength would allow for reasonable count times for assaying rows of pins up to 8-pins per row (20 minute count time). This source strength is also based on the preliminary NRTA system design outlined in reference [1]. An important requirement for these estimates is the use of a segmented flight tube of total length 5-meters, and neutron and gamma shielding strategically placed around the flight tube to eliminate background counts.

The NRTA technique is currently defined and envisioned to be a high-accuracy non-destructive technique; the overall system being a relatively large, non-mobile, fixed installation. Currently the most likely application for the NRTA system would be at the front end of a reprocessing plant for assay spent fuel to determine the total plutonium entering the facility. One significant advantage of the NRTA system is multiplexing the spent fuel throughput by utilizing the NRTA 4π neutron emission. A factor of 10 increase in throughput can be realized by having ten (instead of one) horizontal flight tubes emanating from the source. Additional flight tubes oriented at polar angle above and below the horizontal tubes would allow for multiple axial scans on each assembly, further increasing the assay accuracy and throughput.

NRTA transmission scans can readily identify four plutonium isotopes (^{239}Pu, ^{240}Pu, ^{241}Pu, ^{242}Pu), three uranium isotopes (^{235}U, ^{236}U, ^{238}U), and six resonant fission products (^{99}Tc, ^{103}Rh, ^{131}Xe, ^{133}Cs, ^{145}Nd, and ^{152}Sm). This technique can determine the areal density or mass of these isotopes in single- or multiple-pin integral transmission scans. Published literature suggests an assay accuracy of 1-4% uncertainty for these isotopes. An assembly mass estimate for ^{239}Pu was part of the FY2011 work. For an 8-pin assay capability, it was shown that the NRTA technique (calculated transmission spectra) could estimate the total ^{239}Pu assembly mass to within approximately 4% of the known value using a simplified, straightforward analysis technique. For a 12-pin scan capability, every pin in the assembly could be part of one or more integral scans; in this approach multiple scan information for the same pins could be unfolded to potentially allow the determination of ^{239}Pu mass values for sub-regions of the assembly. Further, the mass estimate accuracy could be greatly improved, perhaps to the 1-2% level, upon

the development of more sophisticated computer analysis tools that could correct the transmission spectra for resonance overlap/interference and hidden resonance within the actinide or fission product resonance of interest. These analysis tools should be straightforward to develop since the resonance structure is now well known and some of these tools have been previously developed for other NRTA-type applications. Also, more sophisticated methods, relative to the "depth" method used here for evaluating the transmission factor (T), could be implemented and developed specifically for the NRTA technique. All these developments would improve the NRTA measurement accuracy.

7 REFERENCES

1 Sterbentz, J.W. and Chichester, D.L., “Neutron Resonance Transmission Analysis (NRTA): A Nondestructive Assay Technique for the Next Generation Safeguards Initiative’s Plutonium Assay Challenge,” Report INL/EXT-10-20620, Idaho National Laboratory, Idaho Falls, Id. (2010).

2 Tobin, S.J., et al., "Next Generation Safeguards Initiative Research to Determine the Pu Mass in Spent Fuel Assemblies: Purpose, Approach, Constraints, Implementation, and Calibration," Nucl. Inst. Meth. Phys. Res. A, doi:10.1016/j.nima.2010.09.064 (in press).

3 Schrack, R.A., et al. “Resonance Neutron Radiography using an Electron Linac,” IEEE Trans. Nucl. Sci. 28 (1981) 1640-1643.

4 Bowman, C.D., et al., “Neutron Resonance Transmission Analysis of Reactor Spent Fuel Assemblies,” *Neutron Radiography*, Barton, J. P. and von der Hardt, P., eds., ECSC, EEC, EAEC, Brussels, Belgium and Luxembourg (1983) 503-511.

5 Behrens, J. W., Johnson, R. G., and Schrack, R. A., “Neutron Resonance Transmission Analysis of Reactor Fuel Samples,” Nucl. Tech. 67 (1984) 162-168.

6 Knoll, G. F., *Radiation Detection and Measurement*, 3rd edition, John Wiley and Sons, Inc., Hoboken, N. J. (2000) Chs. 8, 14, and 15.

7 Gavron, A., Smith, L. E., and Ressler, J. J., “Analysis of Spent Fuel Assemblies using a Lead Slowing Down Spectrometer,” Nucl. Inst. Meth. Phys. Res. A 602 (2009) 581-587.

8 Priesmeyer, H. G. and Harz, U., “Isotopic Assay in Irradiated Fuel by Neutron Resonance Analysis,” Atomkernenergie (ATKE) 25 (1975) 109-113.

9 Noguere, G., et al., “Non-Destructive Analysis of Materials by Neutron Resonance Transmission,” Nucl. Inst. Meth. Phys. Res. A 575 (2007) 476-488.

10 Schrack, R. A., “Uranium-235 Measurement in Waste Material by Resonance Neutron Radiography,” Nucl. Tech. 67 (1984) 326-332.

11 Schrack, R. A., “New Applications of Resonance Neutron Radiography,” International Conference on Nuclear Data for Basic and Applied Science, Santa Fe, N.M., May 13-17 (1985).

12 Johnson, R. G. and Schrack, R. A., “Nondestructive Evaluation of M732 Proximity Fuzes,” Report NBSIR 85-3259, National Bureau of Standards, Gaithersburg, Md., November (1985).

13 Behrens, J. W., Schrack, R. A., and Bowman, C. D., “Nondestructive Examination of a Defective Silver Braze using Resonance-Neutron Radiography,” Nucl. Tech. 51 (1980) 178-182.

14 Schrack, R. A., "U-235 Measurement by Resonance Neutron Radiography," Report RADP/B119 NBS, Final report to the U.S. Nuclear Regulatory Commission, National Bureau of Standards, Gaithersburg, Md., June 30 (1983).

15 Bowman, C. D., "Efficient Neutron Production Using Low-Energy Electron Beams," Proc. Int. Conf. on Nuclear Cross Sections for Tech., Univ. of Tennessee, Knoxville, Tenn., Oct. 22-26 (1980) 531.

16 "*MCNP—A General Monte Carlo N-Particle Transport Code, Version 5*," X-5 Monte Carlo Team, Report LA-UR-03-1987, Los Alamos National Laboratory, Los Alamos, N.M. (2003).

17 "*MCNPX—A General Purpose Monte Carlo Radiation Transport Code, Version 2.5.0*," MCNPX User's Manual, LA-UR-05-0369, Los Alamos National Laboratory, Los Alamos, N.M. (2005).

18 Fensin, M. L., et al., "A Monte Carlo Linked Depletion Spent Fuel Library for Assessing Varied Nondestructive Assay Techniques for Nuclear Safeguards," Report LA-UR-09-01188, Los Alamos National Laboratory, Los Alamos, N.M. (2009).

19 Chadwick, M. B., et al., "ENDF/B-VII.0: Next Generation Evaluated Nuclear Data Library for Nuclear Science and Technology," Nucl. Data Sheets 107 (2006) 2931-3060.

20 Lakosi, L. and Nguyen, C.T., "Neutron Interrogation of High-Enriched Uranium by a 4 MeV Linac," Nucl. Inst. Meth. Phys. Res. B 266 (2008) 3295-3301.

21 Eshwarappa, K.M., et al., "Comparison of Photoneutron Yield from Beryllium Irradiated with Bremsstrahlung Radiation of Different Peak Energy," Ann. Nucl. Energy 34 (2007) 896-901.

22 Auditore, L., et al., "Study of a 5 MeV Electron Linac Based Neutron Source," Nucl. Inst. Meth. Phys. Res. B 229 (2005) 137-143.

23 Berger, M.J. and Seltzer, S.M., "Bremsstrahlung and Photneutrons from Thick Tungsten and Tantalum Targets," Phys. Rev. C 2 (1970) 621-631.

24 Shope, L. A., "Theoretical Thick Target Yields for the D-D, D-T, and T-D Nuclear Reactions Using the Metal Occluders Ti and Er and Energies up to 300 keV," Report SC-TM-66-247, Sandia national Laboratories, Albuquerque, N.M. (1966).

25 Hawkesworth, M. R., "Neutron Radiography: Equipment and Methods," Atomic Energy Rev. 15 (1977) 169-220.

26 References for this section may be found at: www.indiana.edu/~lens/UCANS/.

27 Trellue, H.R., et al., "Description of the Spent Nuclear Fuel Used in the Next Generation Safeguards Initiative to Determine Plutonium Mass in Spent Fuel," Report LA-UR-11-00300, Los Alamos National Laboratory, Los Alamos, N.M. (2010).

28 Behrens, et al., "Resonance Neutron Radiography for Nondestructive Evaluation and Assay Applications," NBS Special Report 594, National Bureau of Standards, Gaithersburg, Md. (1979) 436-439.

29 Taken from the references of Uno, S., et al., at www.indiana.edu/~lens/UCANS/.